University of Twente.

Masterthesis Biomedical Engineering
Developmental BioEngineering

INSULIN-PRODUCING PEG-TA MAPS

Bottom-up Tissue Engineering of Immunoprotected Insulin-Producing Microtissues to Improve Islet Cell Transplantation for Type 1 Diabetes

Keywords:
Insulin; Tissue Engineering; Islet Cell; Microtissues; Poly(EthyleneGlycol); PEG-TA; Tyramine; MIN6; Microgel; Crosslink; MAPS; Microporous Annealed Particles; Type 1 Diabetes Mellitus; Microfluidic Platform; Immunoprotective;

Author
Patrick Vincent Blokzijl

Supervisors
Prof. Dr. J.C.H. Leijten
M.R. Schot Msc.
Dr. N.M. Araújo Da Cunha Gomes

External Committee Member
Prof. Dr. D. Stamatialis
Dr. L.S. Moreira Teixeira

Date
16-09-2022

Contents

Abstract

Type 1 diabetes mellitus (T1DM) is a worldwide spread disease with increasing incidence. It is the ninth leading cause of death, with over 1.5 million deaths in 2019 [1]. T1DM is an autoimmune disease where beta-cells in the pancreas are killed. Beta-cells produce insulin in healthy people whenever the blood-glucose level becomes too high, lowering the blood-glucose level. T1DM patients cannot lower their blood-glucose level anymore without treatment, which is normally administering exogenous insulin. Another option is to get a pancreas or beta-cell transplant.

Beta-cells can be encapsulated in microgels for implantation. However, microgels face retrievability problems and activate a fibrotic response. They can also escape the implant-site, which could be dangerous. Microporous annealed particles (MAPS) are compounds composed of microgels crosslinked to each other. MAPS are very porous, larger particles, combining favorable traits of microgels and macrogels. MAPS are better retrievable than microgels due to their size, while also having a higher diffusability and vascularity potential then macrogels. Besides, MAPS are associated with a reduced fibrotic response compared to microgels. A bottom-up strategy by creating a MAP made from hollow PEG-TA microgels, laden with MIN6 cells, which are able to produce insulin is proposed in this research.

We made monodisperse, hollow, cell-laden microgels using a microfluidic platform which could be crosslinked together via a ruthenium-sodium persulfate crosslink with visible light. Cells aggregated within the microgels and survived for at least 28 days, while growing and filling the hollow space in the microgel. Cells maintained their insulin and glucagon receptors, indicating that the cells remained bioactive. MAPS showed excellent porosity, with poresizes large enough for capillaries and small blood vessels. Diffusion of small molecules over the microgels in the MAP was very fast, while larger molecules like antibodies were blocked.

Although further research is necessary to see if the cells can lower a hyperglycemic situation, we showed that it is possible to create MAPS out of cell-laden microgels with cells maintaining their insulin receptors.

Samenvatting

Type 1 diabetes mellitus (T1DM) is een wereldwijd verspreide ziekte met een toenemende incidentie. Het is de negende belangrijkste doodsoorzaak, met meer dan 1,5 miljoen sterfgevallen in 2019 [1]. T1DM is een auto-immuunziekte waarbij betacellen in de alvleesklier worden gedood. Betacellen produceren bij gezonde mensen insuline wanneer het bloedglucosegehalte te hoog wordt, waardoor het bloedglucosegehalte daalt. T1DM-patiënten kunnen hun bloedglucosespiegel niet meer verlagen zonder een behandeling, die meestal bestaat uit het toedienen van exogene insuline. Een andere optie is een transplantatie van de alvleesklier of betacellen.

Betacellen kunnen worden ingekapseld in microgels voor implantatie. Microgels laten echter problemen zien bij het terughalen van de microgels en activeren een fibrotische reactie. Ze kunnen ook uit de implantatieplaats ontsnappen, wat gevaarlijk kan zijn. Microporeuze samengeklikte deeltjes MAPS zijn zeer poreuze, grotere deeltjes, die positieve eigenschappen van microgels en macrogels combineren. MAPS zijn door hun grootte beter terug te vinden dan microgels, en daarbij hebben ze ook een grotere diffusibiliteit en vascullariteitspotentieel dan macrogels. Bovendien worden MAPS geassocieerd met een verminderde fibrotische respons in vergelijking met microgels. In dit onderzoek wordt een bottom-up strategie voorgesteld door een MAP te maken van holle PEG-TA microgels, geladen met MIN6 cellen, die insuline kunnen produceren.

We maakten monodisperse, holle, met cellen geladen microgels met behulp van een microfluidisch platform die aan elkaar konden worden gekoppeld via een ruthenium-natriumpersulfaat crosslink met zichtbaar licht. Cellen aggregeerden in de microgels en overleefden ten minste 28 dagen, terwijl ze groeiden en de holle ruimte in de microgel opvulden. De cellen behielden hun insuline- en glucagonreceptoren, wat erop wijst dat de cellen bioactief bleven. MAPS vertoonden een uitstekende porositeit, met poriën die groot genoeg waren voor haarvaten en kleine bloedvaten. De diffusie van kleine moleculen over de microgels in de MAP was zeer snel, terwijl grotere moleculen zoals antilichamen werden geblokkeerd.

Hoewel verder onderzoek nodig is om te zien of de cellen een hyperglycemische situatie kunnen verlagen, laten we zien dat het mogelijk is om MAPS te maken van microgels met cellen die hun insulinereceptoren behouden.

Acknowledgements

Last year, I started this project at the DBE group and did not know what I could expect beforehand. I met Maik Schot during a practical and he told me about different projects that I could work on for my thesis. Ultimately I started doing this project with Maik Schot as my supervisor.

During my project, Maik helped me a lot when I got stuck and was always willing to think along. He was there for me everyday and I could always ask anything. I would like to thank Maik for his interest in me and being there when I needed him. He was there for supervision, but also to work along which made experiments more bearable and fun when it did not work immediately. I feel like I learned a lot from him and could not be more lucky with him as my daily supervisor. Thank you very much!

Since my project continued from the work of dr. Nuno Araújo Da Cunha Gomes, he taught me how use the microfluidic setup and showed me around the labs in the Zuidhorst. Nuno was always very friendly and happy to help whenever something went wrong with the microgels. Besides the experiments, he was always willing to make time for me and even supervise me whenever Maik did not have time. I am very grateful for all you have done, thank you Nuno!

I would also like to thank dr. Jeroen Leijten for the opportunity of working with him on this project. Jeroen was always very eager to help and guide me in the right direction. Despite the very full agenda of Jeroen, he always had time for me to talk about the experiments and the project as a whole. Besides giving input, he was also open to listen to me and think along, and also to just have small talk occasionally.

Besides spending time with my supervisors, I also spent a lot of time with other people of the DBE group. I want to thank the PhD candidates of the DBE group for helping me with various experiments, such as teaching me how to work with the rheometer and the nanoindentation. You made my year a lot of fun and inspiring everyday. You really embraced my presence and made me feel like part of the group. I would also like to thank the other students working in the Zuidhorst labs, especially Lucy Tao for helping me with a lot of things, such as mass producing PDMS chips, and being there for each other when needed.

1. *Introduction & Background*

1.1 Type 1 Diabetes Mellitus

Diabetes Mellitus (DM) is a disease in which the body cannot secrete insulin or does not respond appropriately to it [2]. Type 1 Diabetes Mellitus (T1DM) is a chronic autoimmune disease in which the innate and adaptive immune systems attack the pancreatic beta-cells [3], destroying the patient's ability to produce insulin. T1DM is mostly diagnosed during childhood, but contrary to popular believe can also be done during adulthood [4]. The lack of insulin production will result in a high blood glucose level (hyperglycemia) over time. A prolonged elevated blood glucose level can result in severe complications, like loss of vision, kidney failure, and cardiovascular diseases [5].

1.1.1 Pancreatic Beta-Cell Physiology

A healthy individual can synthesize insulin in pancreatic beta-cells, which are a part of the islets of Langerhans. In humans, the islets consist of about 50% beta-cells [6], but also contain other types of cells. Other endocrine cells that are found in the islets are alpha-cells, delta-cells, epsilon-cells and PP-cells, producing glucagon, somatostatin, ghrelin and pancreatic polypeptide, respectively [7]. Besides endocrine cells, there are also stromal cells, vascular cells, immune cells and neural cells to be found in the islets, like fibroblasts, endothelial cells, lymphocytes and neurons, respectively [8]. Synthesis of insulin happens constantly and can be increased or decreased to meet the metabolic demands precisely. Beta-cells can sense the changes in blood glucose levels and regulate their insulin release accordingly [9]. Due to the islet structure of the cells and the excellent vasculature connection, the cells come in contact with 10 times as much blood as other surrounding exocrine regions. Besides the high amount of blood, the capillaries are also very porous. The pores in the capillaries are called fenestrae, which grants a large permeability and fast nutrient exchange, so beta-cells can act rapidly to blood glucose changes [10]. Fenestrae also allow for a fast insulin diffusion to the blood.

Insulin is a peptide hormone consisting of 51 amino acids, weighing 5.8 kDa. It is derived from its precursor preproinsulin which is encoded by the insulin gene. Preproinsulin consists of 110 amino acids, with a hydrophobic N-terminal signal peptide that can interact with cytosolic ribonucleoprotein signal recognition particles [11]. These signal recognition particles make it possible for preproinsulin to translocate across the rough endoplasmatic reticulum. During the translocation, the signal peptide is cleaved by a signal peptidase to make proinsulin [12]. In the endoplasmatic reticulum, several chaperone proteins help fold the proinsulin by forming three disulfide bonds so the three dimensional conformation of the peptide is attained [13]. The proinsulin then moves to the Golgi apparatus where it can enter immature secretory vesicles. During the formation of the secretory vesicles, proinsulin is simultaneously cleaved, leaving insulin and C-peptide. These products are then stored in the secretory vesicles together with other beta-cells products, like amylin [14].

The synthesis of insulin is affected by multiple factors, with glucose metabolism being the most influential physiological event, stimulating gene transcription, mRNA translation and insulin secretion [15].

1.1.2 T1DM Pathophysiology

Diabetic patients have a deficiency of insulin due to an autoimmune reaction towards their own beta-cells. This reaction leads to a decrease in beta-cell mass within the islets of Langerhans, as well as a reduction in the secretory functionality of the remaining beta-cells. The disease is characterized by the presence of antibodies and T-cells that respond to the antigens on the patients' own beta-cells [16]. The antigens are presented via antigen-presenting cells (APCs) that interact with autoreactive CD4+ T lymphocytes. The CD4+ T lymphocytes activate CD8+ T lymphocytes, who will kill the beta-cells. Due to the destruction of the beta-cells, inflammation grows which stimulates macrophages and B lymphocytes. The B lymphocytes will produce autoantibodies, which is often used as a biomarker to diagnose T1DM [2].

Besides the immunologic factors, genetics and the environment are also factors that play a role in the onset of T1DM [17]. Although T1DM often occurs in patients without a history of the disease in their family, the risk for developing diabetes is significantly increased when a family member has been diagnosed with diabetes [18]. Over 50 genetic risk loci have been identified [19], with the main genes susceptible to leading to T1DM coding for human leukocyte antigens (HLA), which are located on chromosome 6 in the major histocompatibility complex (MHC). HLA haplotypes account for around 45% of the genetic risk in developing T1DM [20].

Environmental factors also play a role in the risk of developing T1DM. Evidence of this has mostly been shown by studies with monozygotic twins [21; 18]. Environmental factors that can play a role are viruses, toxins, and nutrients. The precise effects of these factors is still unclear, but it is important to identify them. Viruses, such as enteroviruses [22; 23], can be triggers through the activation of the innate immune system causing inflammation. However, another study shows that enteroviruses can also lower the risk of T1DM [24]. The autoimmune response can also be triggered via molecular mimicry, which happens when an immune response is directed towards antigens of a virus that is very similar to the antigens of the host. In T1DM, molecular mimicry is found with the coxsackie B4 virus. The virus has a P2-C protein that has a similar amino acid sequence as the glutamic acid decarboxylase (GAD65) enzyme found in beta-cells [25; 26]. Although vaccinations show an activation of the innate immune response, they are different than the viruses and vaccinating children show no increased risk for developing T1DM, even when a risk is already present [27].

A person's diet can also influence the development of T1DM, although the magnitude of the impact is still controversial. Cow milk is often associated with an increased risk in T1DM [28], due to a small peptide part found in the albumin in the milk. The peptide can function as a self-reactive epitope, appearing similar to the p69 protein, which can be found on the surface of beta-cells [29]. Besides cow milk, other nutrients that are involved in increasing the risk of T1DM are nitrate in drinking water [30], a lack of vitamin D [31], and cereals in early infancy [32], while an adequate intake of omega-3 fatty acids can lower the risk of T1DM [33].

The gut microbiota is another factor involved with T1DM [34]. Differences in gut microbiota have been found between healthy individuals and patients with T1DM [35; 36]. The cause of the changes is still not fully understood, but even the manner how a baby is born seems to be involved [37]. A cesarean section is associated with an increased risk of developing T1DM, since the baby has not been in contact with the vaginal microbiome of the mother which leads to a difference in gut microbiota [38].

1.1.3 Clinical Implications

The last decades, complications have substantially decreased and outcomes have improved [39]. However, there are still a lot and severe complications that contribute a large part to the mortality rate of T1DM patients. Hypoglycemia and ketoacidosis are still life threatening events. Hypoglycemia happens when the blood-glucose level drops too low. If a person encounters a lot of these events, they can become unaware of them which increases the risk of severe implications [40]. Hypoglycemia is also associated with a decrease in cognitive function [41] and accounts for up to 10% of the deaths related with T1DM [42]. Ketoacidosis is the accumulation of ketones in the blood, which makes the blood acidic. In ketoacidosis, the blood has become too acidic and can lead to death if not treated. Around 15% of T1DM related deaths

is due to ketoacidosis [42]. Hyperglycemia, when the blood-glucose level is too high, can also lead to a lot of complications. Hyperglycemia is extremely bad for the vasculature on micro- and macro-level. Hyperglycemia is associated with retinopathy, neuropathy, nephropathy, but also atherosclerosis and thrombosis in the heart and brain [2]. Cardiovascular complications can shorten the lifespan of T1DM patients by 13 years [43]. Besides T1DM being a severe disability for patients, loved ones of patients also reportedly suffer from the effects caused by T1DM [44]. Fear resides in loved ones that hyper- or hypoglycemic events could happen [45].

1.1.4 Prevalence

Prevalence of T1DM has increased in the last few years. T1DM is a worldwide disease, although some continents show a higher incidence. Africa shows a relative low incidence of 8 per 100.000, while America has an incidence of 20 per 100.000. With the rising amount of people suffering from T1DM, complications also become more frequent. With the current rise of prevalence and incidence of T1DM, insulin and treatment for common complications can become scarce and more expensive, especially in underdeveloped countries. [46]

1.1.5 Other Types of Diabetes

There are multiple types of diabetes. Type 1 and type 2 diabetes mellitus (T2DM) are the main types of diabetes, but there is also gestational diabetes, pre-diabetes, and some more rare types like type 3, 3c, LADA, MIDD, MODY and CFRD but these rarer types will not be explained further since they mostly differ in the situation patients are in or what other diseases they have.

T2DM is the most common form of diabetes, with more than 95% of diabetic patients having T2DM [1]. Patients with T2DM cannot produce enough insulin or the cells of the patients are not responsive to insulin anymore [47]. T2DM is a metabolic disorder instead of an autoimmune disease like T1DM, so T2DM is often treated by changing a persons lifestyle with medication being an extra option to alleviate symptoms, while in T1DM medication being the primary medication and lifestyle changes a second option to relieve symptoms. T2DM is often associated with diagnosis in adulthood, but incidence in children is increasing rapidly [48].

Gestational diabetes occurs exclusively in women, since it occurs during pregnancy. Women with gestational diabetes have hyperglycemia during pregnancy, which normally disappears after giving birth. It can cause serious implications for the woman and baby if not taken care of. People that had gestational diabetes have a higher chance of developing T2DM [49].

When a person has a blood-glucose level above the normal range but not as high as diabetic patients, they can be diagnosed with pre-diabetes. Pre-diabetes increases the risk of developing other types of diabetes [50].

1.2 Current Therapies

When a patient gets diagnosed with T1DM, treatment is necessary to lower the risk of further implications and to remain on the same level of quality of life. Multiple therapies are currently available for T1DM patients, but they are seldom permanent and are mostly relieving the symptoms and avoiding the disease from worsening.

1.2.1 Administration of Exogenous Insulin

Since T1DM is an autoimmune disease towards the beta-cells in the pancreas and not insulin itself, patients can replace their need for insulin with insulin replacement therapy. When in 1922 insulin was discovered, diabetes was no longer terminal but could be treated [51]. Since then, exogenous insulin has improved and can currently mimic endogenous insulin way better [52]. Patients can live long lives by administering exogenous insulin over the day via injections or an insulin pump, but they need to do this for the rest of their lives [53]. Besides a lifelong dependency on exogenous insulin, T1DM patients are more prone to obesity, hypoglycemic events, psychiatric conditions and even insulin resistance over time [54]. Another drawback of a

lifelong dependency on exogenous insulin is the administration, which is an invasive procedure [55].

1.2.2 Lifestyle changes

Often, lifestyle changes are used in combination with insulin replacement therapy. A healthier lifestyle can reduce the dependency on exogenous insulin, but only to a degree in T1DM. The most impactful change is an intensive diet change. By not increasing the blood-glucose level much, insulin dosage can be lowered. However, only changing ones lifestyle cannot cure T1DM, nor can it elevate all symptoms. Other changes that a patient can integrate in their life are stopping with smoking, workout, sleep the recommended amount of hours, and avoid stress [56].

1.2.3 Pancreas transplant

T1DM patients can also be eligible for a pancreas transplant. A pancreas transplant is an alternative for livelong dependency on exogenous insulin by restoring the patient's glucose regulation. However, a pancreas transplant changes the livelong insulin dependency to an immunosuppression dependency in order to not reject the transplanted pancreas. There is also a donor shortage, and in combination with strict donor requirements, patients often need to wait at least a year [57]. Additionally, a pancreas transplant is a major surgery which carries risks. However, due to the high incidence of kidney failures in T1DM patients [58], kidney transplants can often be combined with a pancreas transplant [59]. Combining the transplants does not lower the risk, but it is also not increased.

Islet cell transplant

To lower risks during surgery, an islet cell transplant is also possible instead of a pancreas transplant. After an islet cell transplant, patients still need to take immunosuppression medicine. However, islet cell transplants offer a higher potential for engineering strategies to reduce immunosuppression dependency. Unfortunately, islet cell transplants come with new downsides compared to a pancreas transplant. Often multiple donors are required for an islet cell transplant, due to a lot of cell loss in the process [59]. Islets are only harvested from deceased donors, because glucose intolerance can occur when a living donor donates a part of their islets [59]. Islets are isolated from the pancreas using a Ricordi chamber [60] with the Edmonton protocol [61], which is the standard protocol for islet isolation, and although this protocol has been optimized there is still some cell loss. Immediately after the transplant, an instant blood-mediated inflammatory response (IBMIR) occurs which leads to loss and damage of islets. During the revascularization of the islets, which can take several months, ischaemia occur and viability of islets decreases. Side effects of immunosuppressive agents can lower the viability of the islets even more [62]. To reach insulin independence, a patient needs between 5000-10.000 islets per kilogram bodyweight [63; 64].

A strategy that is being researched to lower or even remove the need for systemic immunosuppression, is the encapsulation of islets so they become immunoprotected [65].

1.3 Islet cell encapsulation

Transplantation of islet cells comes with several problems. If pristine islet cells are transplanted in a patient, the host immune response will react to the islets, leading to an immunosuppression dependency. To circumvent this problem, the cells can be encapsulated so the immune system will not be able to attack the cells directly [65; 66].

1.3.1 Encapsulation methods

Encapsulating the islets can be done using different methods, which will result in different encapsulation scales. Scales range from macro- to nanoscale. Every method and resulting encapsulation scale has their own advantages and disadvantages.

Macroencapsulation

Encapsulation on a macroscale incorporates the encapsulation of multiple islets in a single macrogel [67]. Due to the size and high amounts of islets encapsulated, only one or a few macrogels need to be implanted to reach the desired effect. A macroencapsulation device is characterized by its size, which is between a few millimetres up to several centimetres [68]. Due to its size, the macrodevices are easily trackable and retrievable by failure or inflammation of surrounding tissue [69]. It is even possible to replenish islets if the function decreases. However, there are severe disadvantages, like a fibrotic response and poor vascularization which can lead to a necrotic core [70].

Nanoencapsulation

Nanoencapsulation devices are usually made by placing thin layers of hydrogel over the surface of the islets [71]. Due to the small size difference of nanoencapsulated islets and non-encapsulated islets, the nanoencapsulated islets can be implanted into the liver via the portal vein. Unlike larger devices, nanodevices hardly increase the risk of thrombosis [72]. The liver has a better blood supply than the subcutaneous space, increasing the chance of success [73]. However, the thin layer of protection is limited, making it difficult to ensure immunoprotection [68]. It is also extremely hard to retrieve nanodevices if they fail or trigger the inflammatory response. Lastly, scaling the production of nanodevices to clinical levels is hardly possible, due to each islet coated individually [74].

Microencapsulation

In microencapsulation, small groups of cells (microtissues) are encapsulated in a spherical shape [75]. Microencapsulated devices range in size between the micro- to millimetre size [76]. Encapsulation is often done using hydrogels, although other materials can be used [77]. Originally, microencapsulation was done via droplet extrusion [78], in which small droplets are pushed in a crosslinking bath. Currently, microfluidic encapsulation is mostly used, because devices are relative cheap and modular. Microfluidic devices also allow for excellent control over the size, shape, and the production rate of the microgels [79; 76]. Due to the small size of the microgels, they have a relative large surface to volume ratio, which is favorable for fast diffusion of nutrients and waste products. Another advantage of microgels is the high amount of capsules, which decreases the risk of the total graft failing. Furthermore, implanting small microgels is less risky and invasive then a larger macroencapsulated device. However, the large amount of microgels is also a disadvantage due to the slow production and low scalability. Furthermore, retrieving microgels is, like nanoencapsulated devices, extremely hard [68; 74].

It is also possible to produce microgels with a hollow core, so cells can aggregate within the microgel and have a faster diffusion. The 3D cell aggregate is more biomimetic and allows for a more clinically comparable model [80; 81]. However, producing hollow microgels was a hard, multi-step process [82; 83]. Van Loo et al.[84] developed an easy to use, fast method. Microgels were enzymatically crosslinked from the outside inwards by using horseradish peroxidase (HRP) and hydrogen peroxide to crosslink tyramine bonds, which is more stable and less harmful than other crosslinking methods [85].

1.3.2 Encapsulation materials

The material in which cells are encapsulated has a large influence on the success of the implantation. Different materials have different properties. When microencapsulation started gaining traction for a treatment for diabetes, alginate was used. Alginate is still a very popular material in microencapsulation of beta-cells, and has since been improved by purification and modifications to make the material more biocompatible [76]. Besides alginate, other materials that have been explored for microencapsulation are agarose, gelatin derivatives, and polyethylene glycol (PEG) [86].

PEG-TA as Encapsulation Material

There are several requirements that an encapsulation material ideally meets, like immunoprotection, diffusability, biocompatibility, and stability over time [87].

PEG is widely used for encapsulation of islets [88; 89]. PEG is a versatile material. It is biocompatible, inert, has mechanical properties that resemble soft tissues, and is nanoporous, which gives it immunoprotective properties [72; 88]. Since PEG is a synthetic polymer, it is easier to mass produce and modify than natural polymers like alginate. It does however lack in diffusability, but if the microgel is thin enough cells do not suffer from a low diffusability [90].

PEG can be conjugated with tyramine, PEG-TA, which makes it possible for a single-step, enzymatic outside-in crosslinking [84].

1.4 Microporous Annealed Particles

As stated before, microgels see a huge use throughout the encapsulation of pancreatic islets. Within our research group Developmental Engineering (DBE), we succeeded in reaching a normoglycemic state in mice by implanting them with insulin-producing cells encapsulated in PEG-TA microgels. However, as also stated before, microgels are not perfect and have their disadvantages. It is extremely hard to retrieve the microgels after implantation, and, although the PEG-TA microgels are immunoprotective, a fibrotic response is triggered after implantation. By annealing the microgels together, a porous biomaterial can be formed, a microporous annealed particle (MAP) (Figure 1.1). MAPS are an emerging class of biomaterials [91]. Due to the size of a MAP, it will be easier to retrieve than loose microgels, and the porosity can also strengthen the link between the MAP and the implantation site. The link can be strengthened when vasculature grows in the porous space of the MAP. The porosity of the MAP also ensures a small diffusion distance, despite the size of the compound. MAP scaffolds are also associated with a reduced fibrotic response [92].

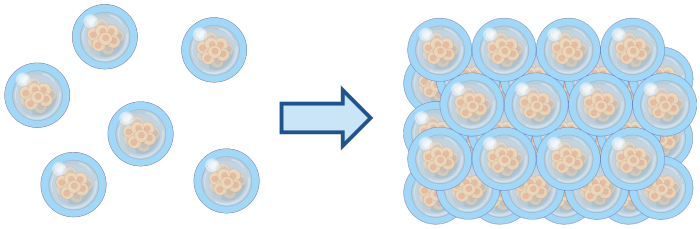

Figure 1.1: Loose microgels can be annealed to form a microporous annealed particle (MAP).

1.5 Problemstatement

Type 1 diabetes is an autoimmune disease in which the body attacks and kills the beta-cells in its own pancreas. Insulin is produced within these beta-cells and is necessary for regulation of the glucose level in blood. Currently, patients need to inject insulin to regain their ability to regulate their glucose level. The incidence and prevalence of T1D is still increasing around the world, so access to insulin for patients will only become harder and less affordable. Other treatments consist of a pancreas or islet cell transplantation, but these still face multiple problems. To improve these treatments, we propose a bottom-up strategy by creating a microporous annealed particle (MAP) made from hollow PEG-TA microgels, laden with cells that are able to produce insulin.

2. *Materials & Methods*

2.1 Microfluidic Droplet Generation

Microgels were made with a microfluidic platform as presented in van Loo et al.[84]

2.1.1 Nozzle Fabrication

Nozzles are made from polyimide-coated fused silica capillary tubing (I.D. 0.20 mm, O.D. 0.36 mm, Polymicro Technologies) by cutting 3 cm parts from the spool. The nozzles are cleaned in a plasma cleaner (FemtoScience CUTE), made hydrophobic with fluorinated silane (Aquapel, Vulcavite), and dried with N_2. The nozzle is partly inserted in a silicone tube (I.D. 0.31 mm, O.D. 0.64 mm, Helix Medica) of around 30 cm, over which a glass capillary spacer (I.D. 0.70 mm, O.D. 0.87 mm, VitroCom) is strung. A droplet of superglue (Bison) is put on the silicone tube at the site where the nozzle is inserted before stringing the glass spacer in place, to keep everything tightly secured.

2.1.2 Droplet Formation Set-Up

A polymer solution was prepared beforehand, containing 10.0% PEG-TA (8-arm, 20 kDa, batch: BZ19005) and 80 U/ml HRP (Sigma Aldrich) in phosphate-buffered saline (PBS). An oil solution was also prepared, comprised of 3.0% Span80 (Sigma Aldrich) in n-Hexadecane (99%, Thermo Scientific). Both solutions are put in different gas tight syringes (Hamilton) and placed on the syringe pump (neMESYS, Cetoni). The solutions are administered to a microfluidic PMMA chip with a T-junction (Figure 2.1) via tubing, with the oil-tubing inserted in the bent part of the T-junction. The nozzle (made as in 2.1.1) is inserted in the last opening of the PMMA chip and is for around 30 cm of the silicone tube of the nozzle submerged in 30% H_2O_2 at room temperature. The syringe pump was set at a flow of 40 µl/min and 8 µl/min for the oil-syringe and polymer-syringe, respectively. See also Figure 2.2 for a schematic.

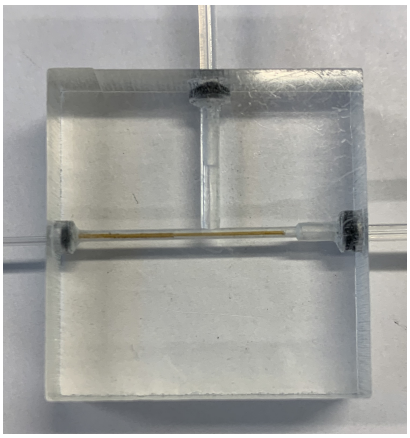

Figure 2.1: Photo of the PMMA chip with the T-junction.

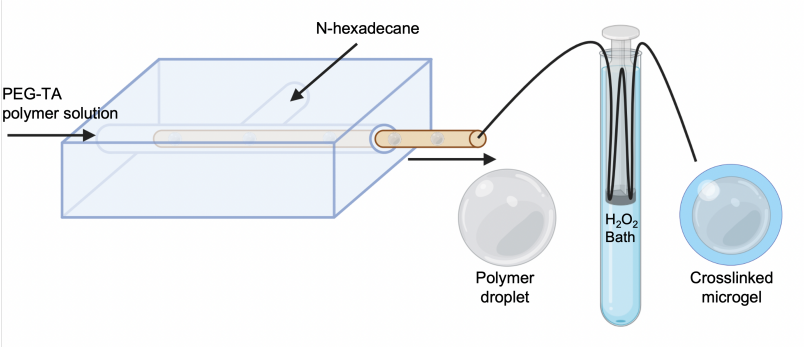

Figure 2.2: Schematic of the Droplet Formation Set-Up; Microgels crosslink from the outside inwards due to the H_2O_2 bath and the HRP in the polymer solution. The silicone tubing on the nozzle is wrapped around a syringe plunger to cover the 30 cm more efficiently.

2.1.3 Cell Encapsulation

The Droplet Formation Set-Up was prepared as described in 2.1.2, except for a few changes due to sterility and the presence of cells. The oil solution was filtered with a 0.2 µm syringe filter. Sterile PBS was added to the HRP and the PEG-TA solution. A small, sterile magnet is inserted in the polymer-syringe before the polymer solution. Cell medium (see 2.4) was prepared with and without fetal bovine serum (FBS). The MIN6 cells were trypsinized and centrifuged and the cell-polymer solution was prepared, containing 10.0% PEG-TA, 80 U/ml HRP, 8.33% OptiPrep (density gradient medium, Sigma Aldrich), and 20.000.000 cells/ml in cell medium without FBS. The cell-polymer solution is put in the gas tight syringe with the magnet and is kept cold during the entire encapsulation. The cell-polymer syringe was used as in 2.1.2.

2.1.4 Washing Microgels

After collecting the product of the Droplet Formation Set-Up with or without cells, the microgels were washed. As much oil-solution was removed from the collection tube as possible and pure n-Hexadecane was added to the collection tube. This is done several times until the microgels are clumped together. After clumping, as much n-Hexadecane as possible is removed and PBS is added. For cell-laden microgels cell medium is used instead of pure n-Hexadecane to wash and is left in the cell medium instead of PBS.

2.2 Microgel Permeability

Microgels with different concentrations of PEG-TA were incubated with 1 mg/ml 150 kDa Immunoglobulin G-fluorescein isothiocyanate (IgG-FITC) (Sigma Aldrich), 10 kDa FITC-dextran (Sigma Aldrich), or 0.4 kDa FITC (Sigma Aldrich) molecules for 24 hours. Images were taken with a confocal laser scanning microscope (Carl Zeiss LSM880) and analysed with FIJI (open source).

2.3 Ethidium Homodimer-1 Staining

Microgels were incubated overnight in ethidium homodimer-1 (EthD-1) at a concentration of 30 µM in PBS. The stained microgels were imaged with a confocal laser scanning microscope (Carl Zeiss LSM880) and analysed with FIJI (open source).

2.4 MIN6 Cell Culture

MIN6 cells were cultured in cell medium, consisting of 10% FBS, 1% penicillin-streptomycin (Pen/Strep) and 6.8 µM β-mercapto-ethanol in Dulbecco's Modified Eagle Medium (DMEM). Cells were passaged when confluency reached 80%. During passaging, cells were trypsinized for 2 minutes at 37 degree Celsius and 5% CO_2. During the experiments, cells with a passage between 33 and 47 were used.

2.5 Cell Viability Analysis

A live/dead staining medium was prepared with calcein AM (live) and EthD-1 (dead) from stock solutions in cell medium (see 2.4). Stock solutions were diluted by 1:4000 and 1:333 for live and dead, respectively. Live/dead staining medium was added to the MIN6 cells or cell-laden microgels and incubated for 40 minutes in 37 degree Celsius and 5% CO_2. Images were taken with a confocal laser scanning microscope (Carl Zeiss LSM880) and analysed with FIJI (open source).

2.6 Cell Morphology Analysis

Cell-laden microgels were fixated using formalin (Sigma Aldrich) on different time-points. A solution of 0.1% Triton X-100 was used to lyse the cells. Microgels were incubated for 30 minutes with 2.5 U/ml phalloidin-AF488 (Molecular Probes) and after washing 10 minutes with 10 µg/ml 4',6-diamidino-2-fenylindool (DAPI) to stain F-actin and DAPI, respectively. Staining the samples was done in a dark room. Stained samples were stored in a fridge. Images were taken with a confocal laser scanning microscope (Carl Zeiss LSM880) and analysed with FIJI (open source).

2.7 Immunofluorescence Analysis

Cell-laden microgels were fixated using formalin after 28 days of incubating. A solution of 0.25% Triton X-100 was used to permeabilize the sample. The sample was blocked with a blocking solution consisting of 1% bovine serum albumin (BSA) in PBS for 20 minutes. The cell-laden microgels were incubated with the primary antibodies mouse anti-insulin (MAB1417) 25 µg/ml and rabbit anti-glucagon (2760S) at 1:200 dilution for 24 hours. After washing, the cell-laden microgels were incubated with the secondary antibodies goat anti-mouse IgG Alexa Fluor 647 (ab150115) at 1:200 dilution and donkey anti-rabbit IgG Alexa Fluor 488 (ab150061) at 1:250 dilution for 1 hour each. The cell-laden microgels were lastly incubated with 1 µg/ml DAPI for 5 minutes. Images were taken with a confocal laser scanning microscope (Carl Zeiss LSM880) and analysed with FIJI (open source).

2.8 Crosslink MAP

Microgels were pipetted in a polydimethylsiloxaan (PDMS) chip on a blanco microscope slide, or on a blanco microscope slide with a cap of a 15 ml tube on top that has a hole in the middle (Figure 2.3). The microgels were crosslinked to a MAP by adding 0.4 mM ruthenium and 4 mM sodium persulfate in the chip, and 1.25 mM ruthenium and 10 mM sodium persulfate with the cap, after which the samples were put under bright, visible light for 10 minutes and 5 minutes whenever the microgels were cell-laden. After crosslinking, samples with the cap were transferred in PBS (or cell medium for cell-laden microgels) and samples in chip were cleaned by pipetting PBS through the chip.

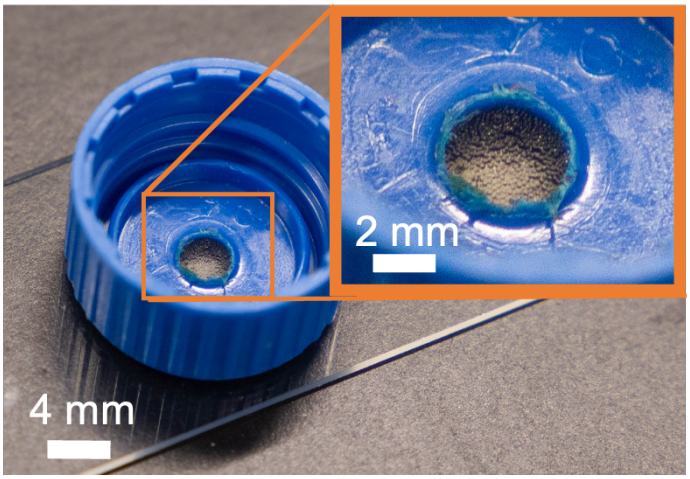

Figure 2.3: Blanco microscope slide with the cap of a 15 ml tube with a hole in the middle. Microgels are deposited in the hole and can be seen.

2.9 Pore Size Distribution

Microgels were fabricated as in 2.1, but PEG-FITC is used in combination with PEG-TA on a 1:20 ratio. Microgels were crosslinked in a chip and imaged with a confocal laser scanning microscope (Carl Zeiss LSM880). The images were analysed with Matlab_R2021a (MathWorks) and FIJI (open source). A simulation with microgels randomly distributed in a box was made in Unity and Blender.

2.10 Hydraulic Conductivity

MAPS and bulk PEG-TA hydrogels were made with the cap on a slider, while a 40 µm filter was glued to the cap (outer side of the cap). A tube filled with water was screwed in the cap so water could flow through the MAP/bulk hydrogel. The amount of water that went through the MAP/bulk hydrogel was measured over time and analysed.

2.11 FluoroBrite Perfusion

A MAP was made in chip. A 0.05% FluoroBrite solution was pumped through the MAP using a microfluidic set-up, similar to set-up presented in Paggi et al.[93]

2.12 Compression Test

MAPS and bulk PEG-TA hydrogels were made with the cap on a slider and stored in a PBS bath in seperate wells. The MAPS and bulk hydrogels were put on a rheometer (Anton Paar Physica MCR 301) and underwent a stress-strain program.

2.13 Rhodamine B Perfusion

MAPS in chip were made and linked to the set-up as presented in Paggi et al.[93]. A solution of 0.1 mg/ml Rhodamine B was attached to an inlet and pumped through the MAP alongside another inlet with milliQ. By changing the flows of the inlets, the presence of rhodamine B or milliQ could be regulated in the MAP.

3. *Results*

3.1 Microgel Characterization

PEG-TA microgels were produced with the microfluidic platform. Different concentrations of PEG-TA were used producing the microgels: 2.5%, 5.0%, and 10.0% PEG-TA. The different microgels were tested on their immunoprotectivity, since this very important when microgels with cells are implanted. An IgG-FITC of 150 kDa was used to test the immunoprotectivity of each microgel with different concentrations PEG-TA. A microgel is said to be immunoprotective whenever it blocks more than 90% of the diffusion over the microgel-shell because then the particle tested is larger than the lowest molecular weight retained by the microgel, the molecular weight cut-off (MWCO). As can be seen in Figure 3.1, a higher concentration of PEG-TA leads to less diffusion of the fluorescent particle into the microgel. The inside of the microgels was compared to the background, which was normalized for all different PEG-TA concentrations. For each PEG-TA concentration, 30 microgels were analysed and averaged with each other. Standard deviation was low for all conditions. The 10.0% PEG-TA microgel blocked the most IgG-FITC, with an average intensity of 8.5%, while the 2.5% and 5.0% PEG-TA microgels had an intensity of 94% and 39% respectively. Since the 10.0% PEG-TA microgel blocked more than 90% (100-8.5=91.5), the 10.0% PEG-TA microgels are immunoprotective. Since this is very important, all other experiments for here on out will be done with the 10.0% PEG-TA microgels.

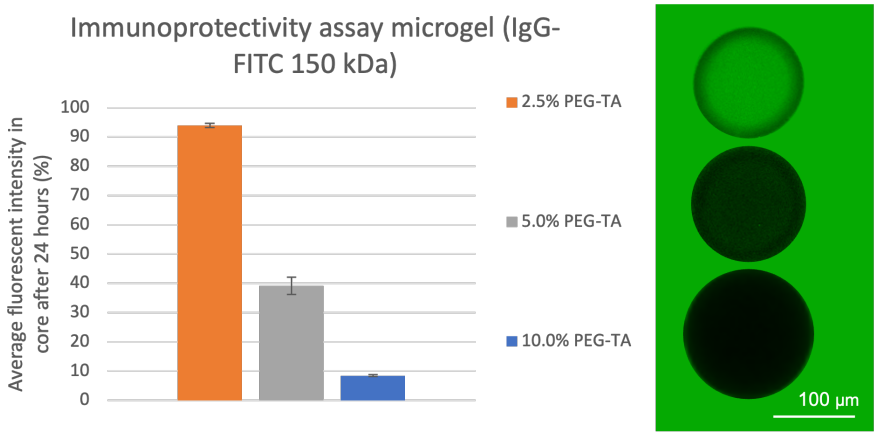

Figure 3.1: Immunoprotectivity assay on microgels with different concentrations of PEG-TA. A visualisation of the diffusion into the microgels is given on the right side, at the same height as the legend. An intensity below 10% is considered immunoprotective. Background intensity was normalized for all microgels. N=30 for all conditions.

Although immunoprotectivity is necessary, the used concentration PEG-TA microgel must still be able to diffuse other molecules, like nutrients, waste, and insulin in and out of the microgel. By using FITC-particles with different molecular weights, specifically chosen for relevance, the diffusability of the microgels could be measured. To mimic the size of glucose, FITC 0.4 kDa was used. Similarly, dex-FITC 10 kDa was used to mimic the size of insulin. Fluorescent intensity was analysed in the same manner as the IgG-FITC. The 10.0% PEG-TA

microgels had a high diffusability for bio-relevant molecules, shown in Figure 3.2. The average intensity for FITC 0.4 kDa was 96% and for dex-FITC 10 kDa 77% after 24 hours.

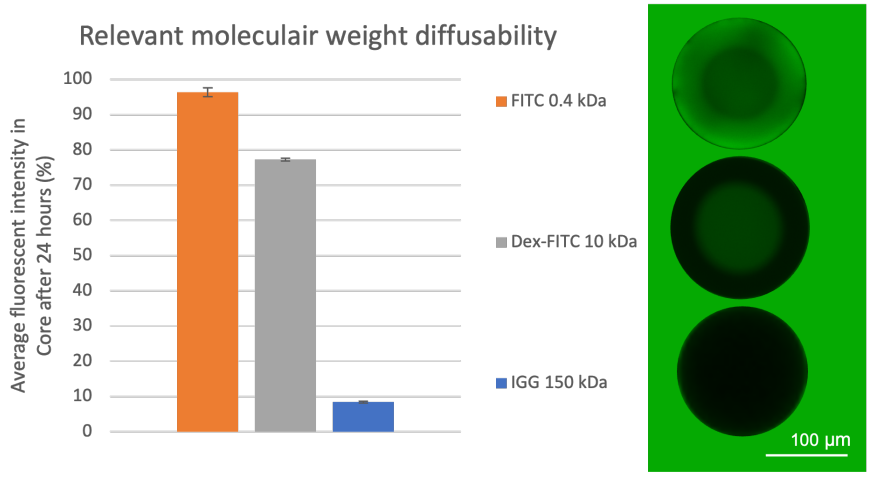

Figure 3.2: Diffusability of bio-relevant molecules. FITC 0.4 kDa and Dex-FITC 10 kDa are similar to glucose and insulin respectively. A visualisation of the diffusion into the microgels is given on the right side, at the same height as the legend. An intensity below 10% indicates a higher molecular mass than the MWCO. Background intensity was normalized for all microgels. N=30 for all conditions.

Since the microfluidic platform runs for some time, microgels cannot be different at the start and the end of the production. The 10.0% PEG-TA microgels were tested on their monodispersity and their size. By adding a EthD-1 staining, the crosslinked tyramine bonds in the shell of the microgel were stained, allowing for an accurate analysis of the size of the microgel and its shell. 30 microgels were analysed. Figure 3.3 shows the distribution of the Feret distance of the microgels, which was approximately 181 µm with a coefficient of variation (CV) of only 1.8%. A CV value lower than 10% is assumed monodisperse, which these microgels are. Since the microgels are hollow, the average size of the shell was also measured, being 29 µm.

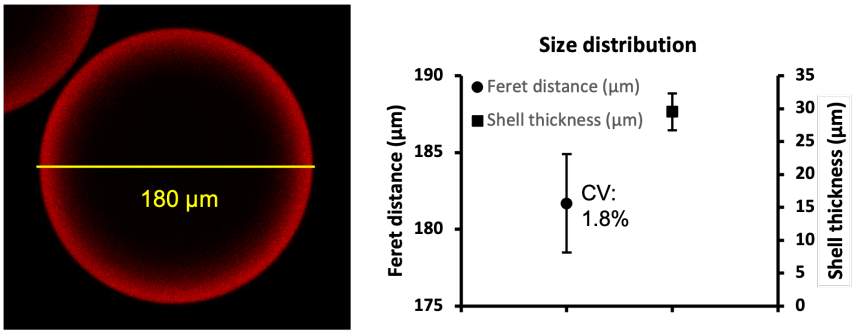

Figure 3.3: Size distribution of the 10.0% PEG-TA microgels. Left: Picture of a single microgel, stained with EthD-1. Right: Feret distance (diameter) of the average microgel in µm with the CV value shown next to it, as well as the average shell thickness. N=30.

3.2 Cell Encapsulation

After the microgels were characterized and the correct concentration of PEG-TA was found, MIN6 cells could be encapsulated. The encapsulation process puts a lot of stress on the cells, so the viability of the encapsulated cells was measured with a live/dead staining. This was done directly after encapsulation (day 0) and on day 1, 7, 14 and 28 after encapsulation. Not encapsulated cells that were still present in the cell-polymer solution were used as a viability

control. Figure 3.4 shows that the encapsulation process in the microfluidic platform was not very stressful, since there is no significant difference between the encapsulated cells and the control on day 0. After a day, cells started to aggregate, so cell viability was not quantifiable anymore. However, Figure 3.4 shows that cells were mostly alive and grew in the microgel over time. The growth of the aggregates in the microgels were analysed by measuring the size of the aggregate on each time point, and was also normalized to the available space in the microgel. The growth stops when the microgel was full and the cells felt the shell of the microgel. After 14 days, the microgels were already almost full, and, as shown in Figure 3.5, the aggregate does not grow much larger. The aggregate does however stretch the shell a bit and puts pressure on the microgel. MIN6 cells are cancerous cells that grow uncontrollably, but the microgels stopped the aggregate growth after 14 days almost completely. This means that the microgels probably work like size limiters for the aggregate inside.

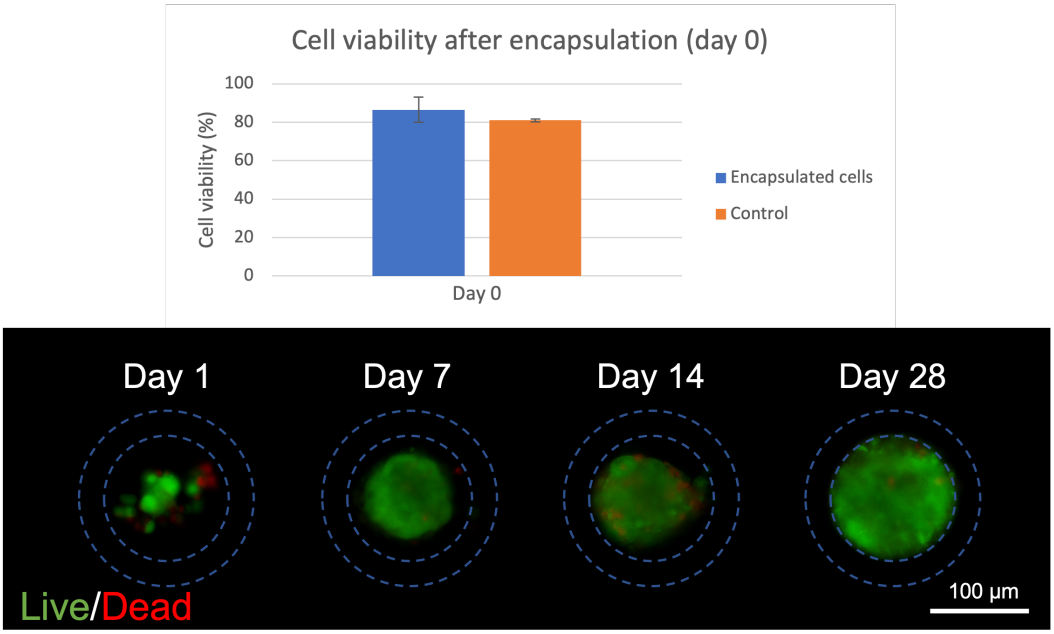

Figure 3.4: Cell viability over time. Day 0 is quantified, other days are qualitative measurements due to aggregation of cells. The ring around the aggregates resembles the size of the microgels inner and outer shell. Live/dead staining was used, green=live; red=dead.

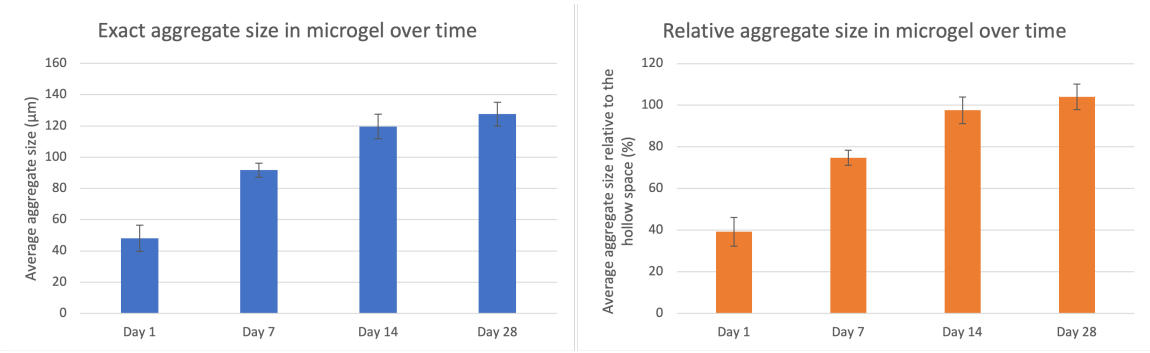

Figure 3.5: Aggregate size over time, exact and relative. Relative size was normalized to the average size of the hollow microgel. N=30.

Because the aggregate puts pressure on the inner shell of the microgel, a possibility arises that the aggregate breaks the microgel from the inside when the aggregate grows larger and the

microgel does not limit the size. Microgels with cells inside were counted on each time point and compared with the amount of cell-laden microgels on day 0. Figure 3.6 shows that the gels with cells inside stay intact over time. Even after 28 days, 94.4% of the gels were intact. So, the microgels did almost not break after 28 days and kept the size of the aggregates at bay, meaning that these microgels are size limiters for the aggregates, even when cancerous cells that aggressively grow are encapsulated. Also, not all microgels encapsulated cells. The amount of cell-laden microgels was compared to the total amount of microgels on day 0, and 92.5% of the microgels had cells in them directly after encapsulation, as can be seen in Figure 3.7.

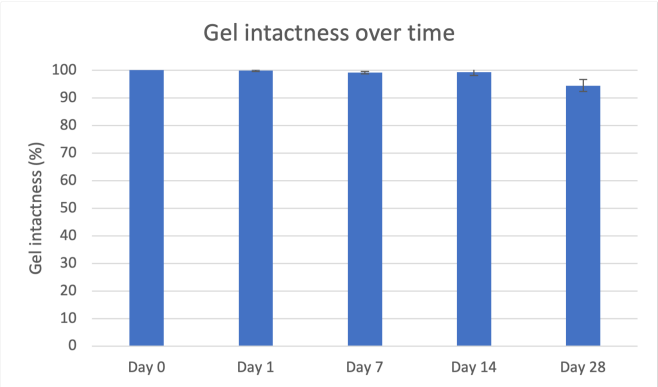

Figure 3.6: Intactness of microgels over time. All days were normalized to day 0 as 100%. N=938.

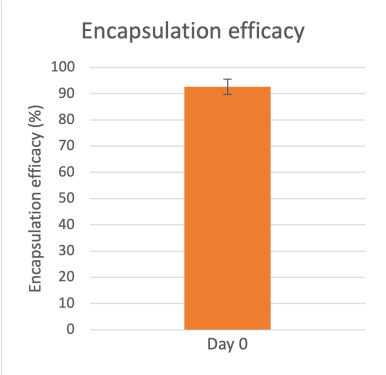

Figure 3.7: Microgels filled with cells relative to the total amount of microgels directly after encapsulation. N=2730.

Since the aggregate fills the hollow space in the microgel over time, the cellular organization within the microgel was tested. Phalloidin/DAPI staining was used on day 1, 7, 14 and 28 after encapsulation to show the cell morphology. In Figure 3.8 an equal distribution of the cells and a growing cytoskeleton over time can be seen.

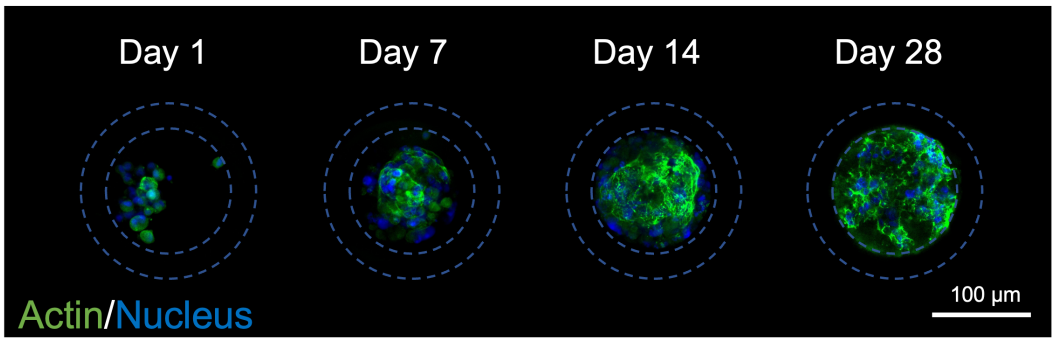

Figure 3.8: Phalloidin/DAPI staining for the F-actin and nucleus of the cells in the aggregate. The ring around the aggregates resembles the size of the microgels inner and outer shell. Green=F-actin/phalloidin; blue=nucleus/DAPI

To see whether the MIN6 cells were still bioactive, an immunofluorescence staining was performed on the glucagon and insulin receptors of the cells after 28 days of culture. Glucagon receptors are stained green and insulin receptors stained red. As shown in Figure 3.9, cells seem still bioactive, because both receptors were still present on the cells (left glucagon, right insulin). DAPI was also used to stain the nuclei, which is colored blue. Although Figure 3.9 shows only one microgel, all cell-laden microgels showed similar results. The glucagon receptor seems more abundant than the insulin receptor, but this could also be due to the weaker signal of the staining.

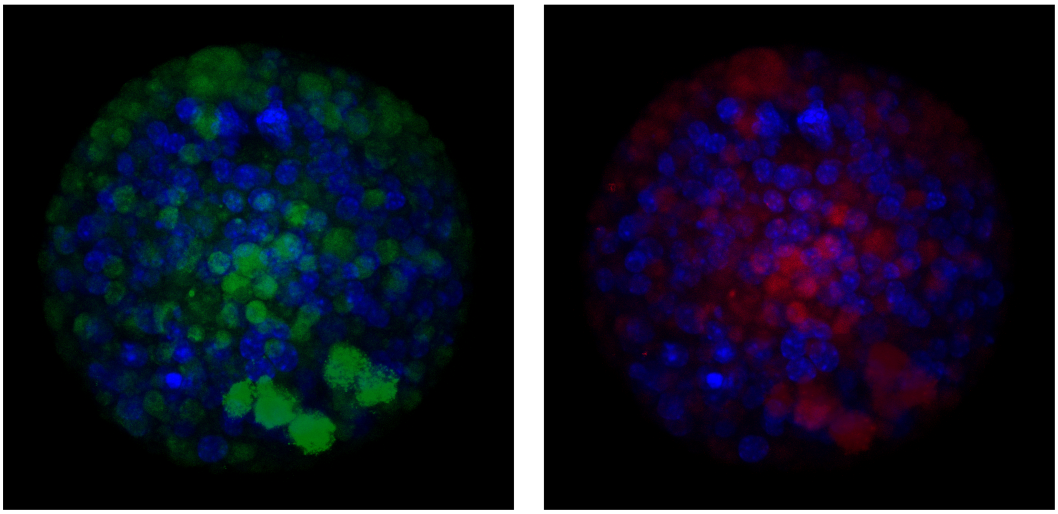

Figure 3.9: Immunofluorescence staining. Both pictures show the same microgel after 28 days of culture. Left: Green color shows presence of glucagon receptors. Right: Red color shows presence of insulin receptors. Blue=nucleus/DAPI.

3.3 MAP Characterization

Before cell-laden MAPS were produced, the MAPS needed to be characterized like the microgels. MAPS were made in two different ways as discussed in 2.8 Crosslink MAP. Because the microgels undergo a second crosslink, immunoprotectivity of the MAP was tested again, see Figure 3.10. This was done similarly as with the microgels, but the MAP was made in a chip and the IgG-FITC was pipetted in the chip afterwards. Both conditions were normalized to the background. The MAP shows an increase in the intensity which becomes higher than 10% (13.3%). This means that the MAP is no longer immunoprotective.

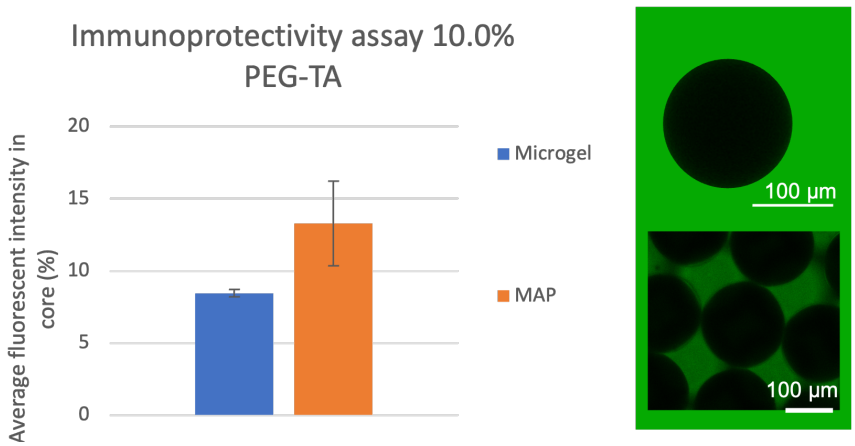

Figure 3.10: Immunoprotectivity assay on a MAP. A visualisation of the diffusion into the microgels is given on the right side, at the same height as the legend. An intensity below 10% is considered immunoprotective. Background intensity was normalized for all microgels. N=30 for all conditions.

An important characteristic of a MAP is the porosity. A big advantage of MAPS are the pores in which capillaries and small blood vessels can grow, but the pores must be large enough for the vessels. Figure 3.11 shows the distribution of poresizes, with pores in the range of 40 to 70 µm being the most abundant. This falls within a relevant range for cell migration and is wide enough to form capillaries and small blood vessels [94]. This gives the possibility for forming a vascular network when implanted, so encapsulated cells have access to exchange nutrients and

waste with the blood. A vascular network can also mean that the MAP is being hold in its place. The packing efficiency was also measured by extracting the volume occupied by the MAP from the total volume measured, which was 65% in the MAP and 63% in the simulated random packing experiment (not shown). This is in line with the 64% packing efficiency associated with randomly poured spheres [95]. This means that a favorable poresize distribution can be achieved with random packing, so microgels do not have to be packed in a certain way.

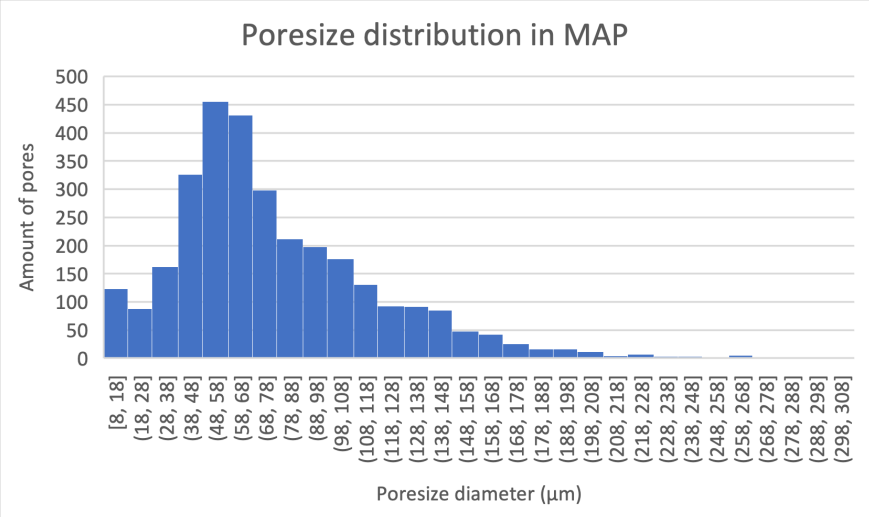

Figure 3.11: MAP porosity histogram. Poresize distribution with most pores being around the 50 µm size which is large enough to sustain a vascular network. N=3060.

As the MAP is proven to be very porous, the hydraulic conductivity was measured, compared to a bulk hydrogel of 10.0% PEG-TA. The hydraulic conductivity is a measurement that describes the ease a fluid can move through the pore space of an object. Since the MAP is a hydrogel, water can move through the polymer network. The hydraulic conductivity was measured by the amount of demineralized water that went through the hydrogel over time. For both conditions, three hydrogels were used that were tested in triplo. Figure 3.12 shows the hydraulic conductivity of the MAP against the nanoporous bulk hydrogel. The average hydraulic conductivity of the MAP was 0.2 µm/s, while the hydraulic conductivity of the bulk hydrogel was $2.1*10^{-5}$ µm/s. The MAP was approximately 10.000 times more easy for water to move through. There was however a large standard error over the hydraulic conductivity of the MAP, but each MAP individually had a much lower standard error (Figure 3.12, smaller graph), meaning that the hydraulic conductivity can largely change between MAPS. The large difference of the hydraulic conductivity between MAPS can be explained by the random packing of the microgels, creating different pore pathways in each MAP. The pore pathways were visualized by flushing a FluoroBrite solution through the MAP. This was done with a MAP in chip. The FluoroBrite particles flow around the microgels, as can be seen in Figure 3.13.

Since the MAP is a porous compound, it could be possible that there is some elasticity compared to a bulk hydrogel. A compression test was performed in triplo to show the stress-strain curve of both compounds, Figure 3.14. The stress-strain curve of the bulk hydrogel pellet goes exponential, which is expected for a hydrogel material, while the curve of the MAP seems to have a bump around 3% strain. The stress-strain curve of the MAP is also flat until 10% strain, while the bulk hydrogel curve is already going up. This looks like there is some displacement in the first 3% strain in the MAP, after which it looks like it behaves elastic up to 10% strain. An elastic region could be beneficial during and after implantation, lowering the chance of breaking the MAP and making it easier to handle.

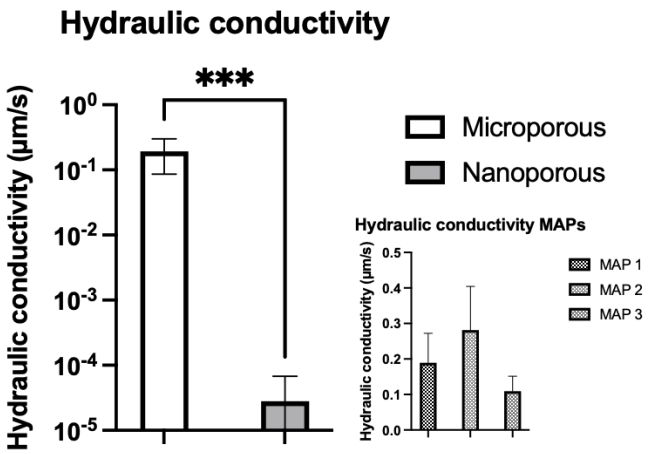

Figure 3.12: Hydraulic conductivity between microporous MAPS and nanoporous bulk hydrogels. There is a significant difference between the MAPS and bulk hydrogel in hydraulic conductivity. In the lower right corner hydraulic conductivity of the different MAPS is shown.

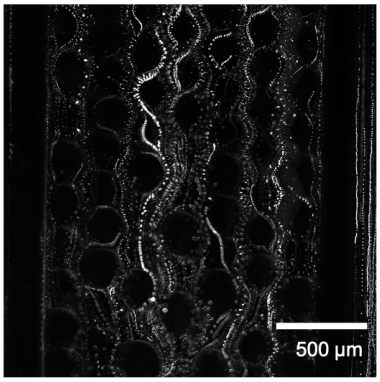

Figure 3.13: Visualization of the pore pathways in the MAP. Illuminated spots are FluoroBrite particles flowing around the microgels in the MAP.

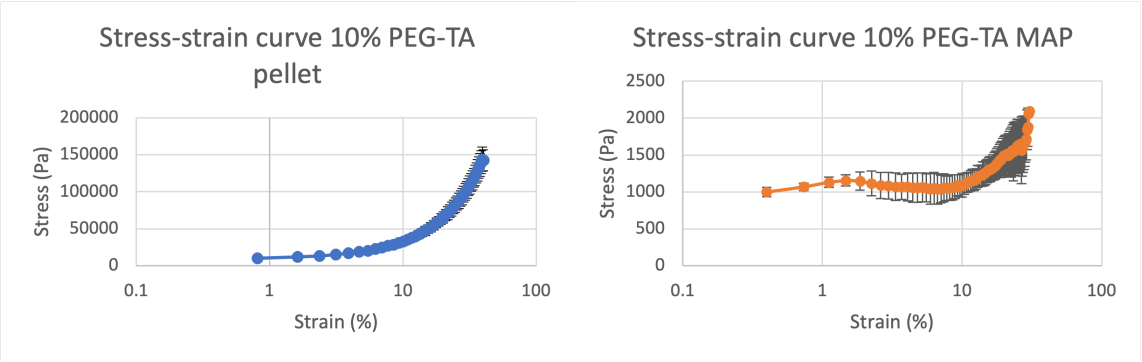

Figure 3.14: Stress-strain curve of 10.0% PEG-TA bulk hydrogel and MAP. Bulk hydrogel behaves like expected, while MAP has a slight bump and flat region up to 10% strain. Both experiments were performed in triplo.

As the MAP has been characterized on a micro (immunoprotectivity) and macro (poresize distribution, hydraulic conductivity, and stress-strain) level, the next experiment will combine these levels in the pore space and diffusability of the MAP. A Rhodamin B solution is flowing parallel with milliQ through a MAP (Figure 3.15). By changing flow rates, the equilibrium between the two solutions is disturbed, moving the border to the left (Rhodamin B solution flows harder) or right (milliQ flows harder) oriented as in Figure 3.15. Changing the equilibrium from left to right and back over a short period of time, causes the Rhodamin B to diffuse in and out of the microgels in the MAP. The fluorescent intensity of the Rhodamin B in microgels on the equilibrium is measured and compared to the background over time. Figure 3.16 shows the relative intensity of the Rhodamin B in the microgels compared with the equilibrium change, where 100% means that at that moment the equilibrium was in favor of Rhodamin B surrounding the microgels with Rhodamin B solution, and 0% means that this was the case with milliQ. Figure 3.16 shows that the Rhodamin B diffuses extremely fast, within a few seconds, in and out of the microgels. The fast equilibrium change shows again that the MAP is highly porous and fluid can easily flow through the pores.

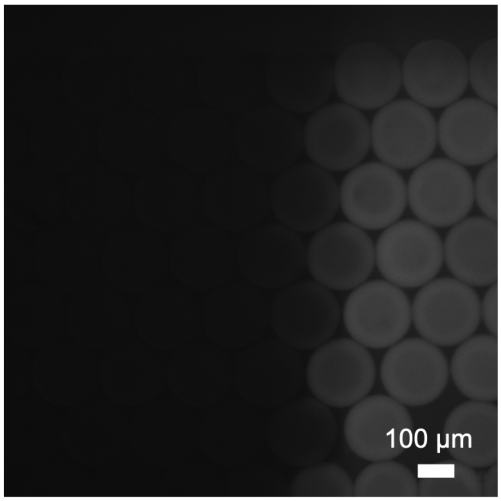

Figure 3.15: Picture of the Rhodamin B and milliQ solutions being in equilibrium. The fluids flow in from the bottom of this picture to the top. Equilibrium moves to the right when milliQ flows harder and to the left when Rhodamin B flows harder.

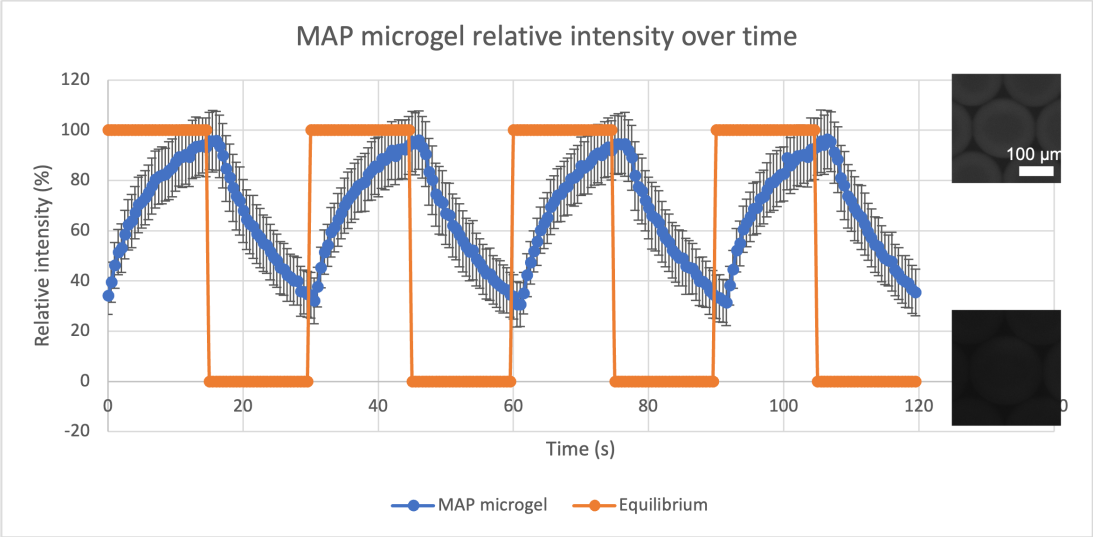

Figure 3.16: Relative Rhodamin B intensity in MAP over time, normalized to the background. Equilibrium at 100% means that it was in favor of Rhodamin B (background was Rhodamin B) and at 0% this was the case for milliQ. On the right are pictures of a MAP microgel with and without Rhodamin B.

3.4 Cell-Laden MAP

Cell-laden MAPS were made by crosslinking the encapsulated cells. Since the encapsulation did not seem to influence viability much, the MAP crosslink was done directly after encapsulation. This extra crosslink could be very stressful because radical sulfate anions come free in the crosslink reaction. The viability of the cells in the MAP were researched with a live/dead staining directly after MAP crosslink and 1, 7, 14 and 28 days after the MAP crosslink. Again, only on day 0 (day the MAP was crosslinked) could the viability quantitatively be measured, due to aggregation of the cells after a day. The viability of the encapsulated cells was used as a control, and Figure 3.17 shows that there is no large difference. The MAP

crosslinked cells had a viability of 79.1%, which is a bit lower than the 83.6% viability of the microgel cells. Figure 3.17 also shows that the aggregates in MAP grow similarly as in the microgels. Over time, the aggregate fills the available space within the MAP microgels.

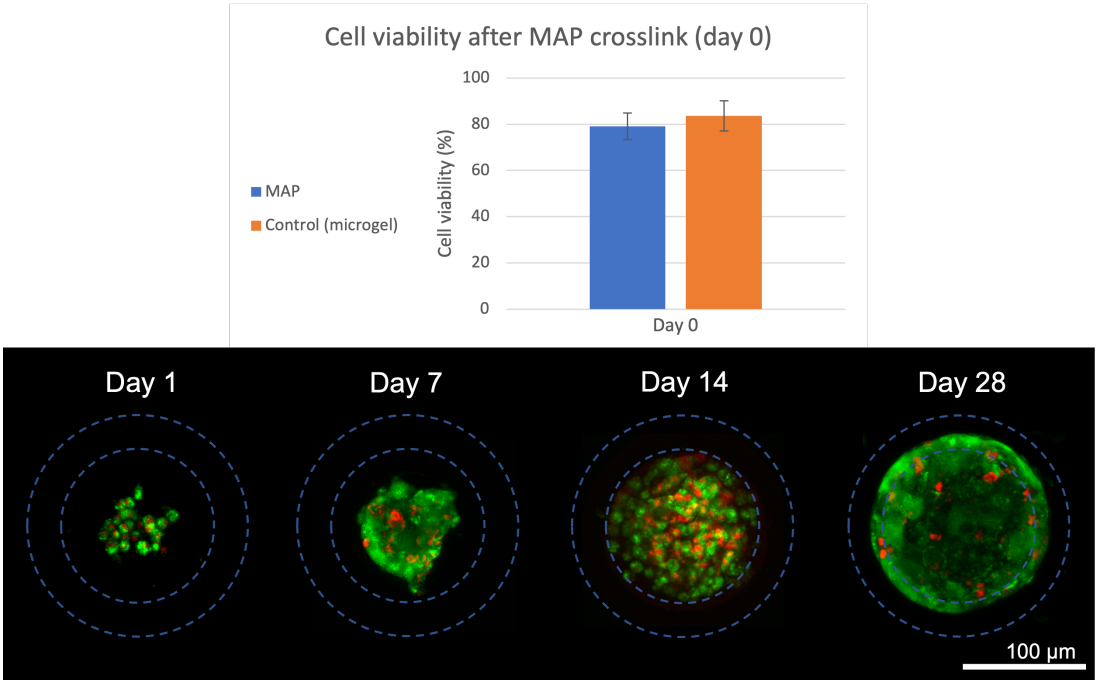

Figure 3.17: Cell viability of a MAP over time. Day 0 is quantified, other days are qualitative measurements due to aggregation of cells. The ring around the aggregates resembles the size of the microgels inner and outer shell. Live/dead staining was used, green=live; red=dead.

4. *Conclusion*

We were able to produce very monodisperse microgels. The microgels were immunoprotective, but could still diffuse bio-relevant molecules. Furthermore, cells could be encapsulated in the microgels with a high viability and continued to grow for at least a month. After 14 days, most hollow space was occupied, which did not change in another 14 days. Meaning that the microgels operate as size limiters of the cell aggregates. Microgels were also mostly intact after 28 days, and aggregates showed presence of glucagon and insulin receptors.

Microgels could be crosslinked with each other to make MAPS. MAPS' immunoprotectivity seems to degrade a bit after crosslinking. The MAPS are porous, with pores the size of capillaries and small blood vessels, which was in line with the random sphere simulation with same size spheres. The diffusability for small molecules was still high and very responsive. It was also possible to incubate cell-laden MAPS for 28 days.

We show that it is possible to create cell-laden MAPS, with cells that have insulin receptors using a bottom-up strategy.

5. *Discussion*

The aim of this study was to create PEG-TA MAPS with insulin-producing cells in the microgels of which the MAP was built. Although we did not measure the insulin production, we showed that the cells after encapsulation maintained their insulin receptors which could mean that the cells are still bioactive. We also succeeded in making a cell-laden MAP that survived for at least 28 days, and during that time grew within the borders of the microgels. The microgels also worked as size limiters for the aggregates. This trait can be explored further with other cell types, since 3D, monodisperse aggregates are hard to create with other techniques. The microgels can also be tuned for other sizes, as the size depends on flow rates within the microfluidic platform system [84].

Most of the results were positive and in line with what we already knew or expected. However, the decrease in immunoprotectivity after the MAP crosslink was unexpected (Figure 3.10), because the MAP crosslink works on the remaining tyramine bonds not crosslinked by the microgel fabrication, meaning that the microgels in the MAP will be crosslinked more than normal microgels. So we would expect that the immunoprotectivity would be better than before. One reason why the immunoprotectivity was worse could be the method used to analyse the microgels. The MAP was made in chip and had multiple layers of microgels, and due to their hollowness a bleedthrough effect was observed. This could mean that the inside of the microgels was in fact darker and the MAP was still immunoprotective. Another result that stood out was the stress-strain curves of the MAP and the bulk hydrogel (Figure 3.14), because the curve of the MAP was different than a standard hydrogel. The flat region could be an elastic region, however, we did not look at this any further. To test if there is an elastic region in the stress-strain curve of the MAP, further research needs to be done. An experiment in which the rheometer strains the MAP for up to 10% and then goes back to 0% for multiple times could measure the elastic property of the MAP. In this case, the stress-strain graph should be a flat line during every cycle.

In this study, MAPS with a maximum size of 12.6 mm^3 were made. However, for there to be enough insulin producing cells, the MAP should be larger. For an islet allotransplant, around 11.000 islet equivalents (IEQ) per kg bodymass is needed [96]. One IEQ is approximately a 150 µm diameter sphere [97], or approximately one cell-laden microgel. This means that a person of 70 kg needs 770.000 IEQ, or 770.000 cell-laden microgels, transplanted to restore normoglycemia. One microgel with a diameter of 180 µm has a volume of $\frac{4}{3} * \pi * 0.090^3 = 0.00305$ mm^3. Since the random packing density of spheres in literature is 64% [95] and we also saw this in our own measurements, the total volume of the MAP needs to be adjusted to the random packing density. This means that the total volume of a MAP with enough IEQ to restore normoglycemia for a person of 70 kg needs to be $\frac{number\ of\ microgels * microgel\ volume}{0.64} = \frac{770.000 * 0.00305}{0.64} = 3673.9$ mm^3. This would be about 300 times larger than we made. The largest challenge would be creating enough cell-laden microgels, since this large amount of microgels needs a lot of cells before encapsulation. Another challenge would be the MAP crosslinking, because this is done with visible light. Enough light needs to go into the MAP without giving off the energy to outer microgels. If the MAP is not crosslinked homogeneously, it can break easily and cells in microgels that were crosslinked more could die due to the radical sulfate anions. Beside these problems, the encapsulation method should be improved before attempting these large amounts of cell-laden microgels. Due to the nature of the MIN6 cells, aggregation started

immediately while in the cell-polymer solution in the syringe. Encapsulation of the cells needs to be done as fast as possible, while keeping the cell-polymer solution cold, to minimize the effect of aggregation of the cells, making it hard to encapsulate large amounts of cells at a time. Tuning the microfluidic platform for encapsulation was also difficult due to aggregation problems. One way to improve the encapsulation process is to use a flow focusing, PDMS chip to avoid problems caused by the interaction of the cell-polymer solution and the nozzle.

Before the production of these many cell-laden microgels for a large MAP is a problem, other unknowns need to be researched. Although the insulin receptors were present in encapsulated cells, we did not test the glucose responsiveness of the cells. This needs to be tested first, with cell-laden microgels and cell-laden MAPS. Another experiment that could be performed is the blood immune response towards the MAP, and whether whole blood can be flowed through the MAP without blood vessels. By testing the blood immune response, a prediction can be done on the fibrotic response to the MAP when implanted [98]. In our group, we also found that PEG-TA microgels could be non coagulant, but this still needs to be explored further with these MAPS.

The most important unknown is the bioactivity of the cells in the MAP. If the cells are still responsive to glucose and can produce and secrete insulin, MAPS can be tested *in vivo* next. Cell-laden MAPS should be implanted in diabetic mice to test the normoglycemic potential of the MAPS. Besides the glucose responsiveness of the MAP, retrievability and fibrosis should also be tested. Retrievability and the amount of fibrosis can also be tested with MAPS without cells, making it possible to test this in normal mice instead of diabetic mice. Other *in vivo* experiments could consist of various tests on immunoresponses, like stainings for various cytokines after implantation or immunohistochemistry to check inflammation in surrounding tissues.

When more experiments have been performed to fill in the last data, and cell encapsulation has been improved and scaled up, the cell type needs to be changed before clinical translation. Currently, MIN6 cells are used for encapsulation. MIN6 cells were derived from mouse insulinoma and are thus cancerous. They were used because of their rapid growth and glucose responsiveness up to 60 passages [99]. Other cell sources that could be used in the clinical translation are differentiated iPSCs, allogeneic islets or xenogeneic islets. Because the microgels are immunoprotective, there would be no problem with different cells, and even autologous differentiated iPSCs could be used. Although these cells will not grow as fast as the MIN6 cells, and fill up the space in the microgel slower, MAPS can be cultured before implantation, or even microgels can be crosslinked on a later time if necessary.

Bibliography

[1] Diabetes;. Available from: https://www.who.int/news-room/fact-sheets/detail/diabetes.

[2] DiMeglio LA, Evans-Molina C, Oram RA. Type 1 diabetes. Lancet (London, England). 2018 6;391(10138):2449–2462. Available from: https://pubmed.ncbi.nlm.nih.gov/29916386/. doi:10.1016/S0140-6736(18)31320-5.

[3] Hull CM, Peakman M, Tree TIM. Regulatory T cell dysfunction in type 1 diabetes: what's broken and how can we fix it? Diabetologia. 2017 10;60(10):1839–1850. Available from: https://pubmed.ncbi.nlm.nih.gov/28770318/. doi:10.1007/S00125-017-4377-1.

[4] Rogers MAM, Kim C, Banerjee T, Lee JM. Fluctuations in the incidence of type 1 diabetes in the United States from 2001 to 2015: a longitudinal study. BMC medicine. 2017 11;15(1). Available from: https://pubmed.ncbi.nlm.nih.gov/29115947/. doi:10.1186/S12916-017-0958-6.

[5] Melendez-Ramirez LY, Richards RJ, Cefalu WT. Complications of type 1 diabetes. Endocrinology and metabolism clinics of North America. 2010 9;39(3):625–640. Available from: https://pubmed.ncbi.nlm.nih.gov/20723824/. doi:10.1016/J.ECL.2010.05.009.

[6] Cabrera O, Berman DM, Kenyon NS, Ricordi C, Berggren PO, Caicedo A. The unique cytoarchitecture of human pancreatic islets has implications for islet cell function. Proceedings of the National Academy of Sciences of the United States of America. 2006 2;103(7):2334–2339. Available from: https://pubmed.ncbi.nlm.nih.gov/16461897/. doi:10.1073/PNAS.0510790103.

[7] Jansson L, Barbu A, Bodin B, Drott CJ, Espes D, Gao X, et al. Pancreatic islet blood flow and its measurement. Upsala journal of medical sciences. 2016 4;121(2):81–95. Available from: https://pubmed.ncbi.nlm.nih.gov/27124642/. doi:10.3109/03009734.2016.1164769.

[8] Huising MO. Tuning to the right signal. Diabetologia. 2015 6;58(6):1146–1148. Available from: https://pubmed.ncbi.nlm.nih.gov/25810040/. doi:10.1007/S00125-015-3567-Y.

[9] Schmitz O, Rungby J, Edge L, Juhl CB. On high-frequency insulin oscillations. Ageing research reviews. 2008 12;7(4):301–305. Available from: https://pubmed.ncbi.nlm.nih.gov/18583199/. doi:10.1016/J.ARR.2008.04.002.

[10] Suckale J, Solimena M. Pancreas islets in metabolic signaling–focus on the beta-cell. Frontiers in bioscience : a journal and virtual library. 2008 5;13(18):7156–7171. Available from: https://pubmed.ncbi.nlm.nih.gov/18508724/. doi:10.2741/3218.

[11] Egea PF, Stroud RM, Walter P. Targeting proteins to membranes: structure of the signal recognition particle. Current opinion in structural biology. 2005;15(2):213–220. Available from: https://pubmed.ncbi.nlm.nih.gov/15837181/. doi:10.1016/J.SBI.2005.03.007.

[12] Patzelt C, Labrecque AD, Duguid JR, Carroll RJ, Keim PS, Heinrikson RL, et al. Detection and kinetic behavior of preproinsulin in pancreatic islets. Proceedings of the National Academy of Sciences of the United States of America. 1978;75(3):1260–1264. Available from: https://pubmed.ncbi.nlm.nih.gov/206890/. doi:10.1073/PNAS.75.3.1260.

[13] Huang XF, Arvan P. Intracellular transport of proinsulin in pancreatic beta-cells. Structural maturation probed by disulfide accessibility. The Journal of biological chemistry. 1995 9;270(35):20417–20423. Available from: https://pubmed.ncbi.nlm.nih.gov/7657617/. doi:10.1074/JBC.270.35.20417.

[14] Steiner DF. The Biosynthesis of Insulin. In: Seino Susumu
}and Bell GI, editor. Pancreatic Beta Cell in Health and Disease. Tokyo: Springer Japan; 2008. p. 31–49. Available from: https://doi.org/10.1007/978-4-431-75452-7_3. doi:10.1007/978-4-431-75452-7_3.

[15] Poitout V, Hagman D, Stein R, Artner I, Robertson RP, Harmon JS. Regulation of the insulin gene by glucose and fatty acids. The Journal of nutrition. 2006;136(4):873–876. Available from: https://pubmed.ncbi.nlm.nih.gov/16549443/. doi:10.1093/JN/136.4.873.

[16] Fu Z, Gilbert ER, Liu D. Regulation of Insulin Synthesis and Secretion and Pancreatic Beta-Cell Dysfunction in Diabetes. Current diabetes reviews. 2013 1;9(1):25. Available from: /pmc/articles/PMC3934755//pmc/articles/PMC3934755/?report=abstracthttps://www.ncbi.nlm.nih.gov/pmc/articles/PMC3934755/. doi:10.2174/15733998130104.

[17] Paschou SA, Papadopoulou-Marketou N, Chrousos GP, Kanaka-Gantenbein C. On type 1 diabetes mellitus pathogenesis. Endocrine Connections. 2018 1;7(1):R38. Available from: /pmc/articles/PMC5776665//pmc/articles/PMC5776665/?report=abstracthttps://www.ncbi.nlm.nih.gov/pmc/articles/PMC5776665/. doi:10.1530/EC-17-0347.

[18] Beyan H, Riese H, Hawa MI, Beretta G, Davidson HW, Hutton JC, et al. Glycotoxin and Autoantibodies Are Additive Environmentally Determined Predictors of Type 1 Diabetes: A Twin and Population Study. Diabetes. 2012 5;61(5):1192. Available from: /pmc/articles/PMC3331747//pmc/articles/PMC3331747/?report=abstracthttps://www.ncbi.nlm.nih.gov/pmc/articles/PMC3331747/. doi:10.2337/DB11-0971.

[19] Størling J, Pociot F. Type 1 Diabetes Candidate Genes Linked to Pancreatic Islet Cell Inflammation and Beta-Cell Apoptosis. Genes. 2017 2;8(2). Available from: /pmc/articles/PMC5333061//pmc/articles/PMC5333061/?report=abstracthttps://www.ncbi.nlm.nih.gov/pmc/articles/PMC5333061/. doi:10.3390/GENES8020072.

[20] Aly TA, Ide A, Jahromi MM, Barker JM, Fernando MS, Babu SR, et al. Extreme genetic risk for type 1A diabetes. Proceedings of the National Academy of Sciences of the United States of America. 2006 9;103(38):14074. Available from: /pmc/articles/PMC1563993//pmc/articles/PMC1563993/?report=abstracthttps://www.ncbi.nlm.nih.gov/pmc/articles/PMC1563993/. doi:10.1073/PNAS.0606349103.

[21] Redonclo MJ, Rewers M, Yu L, Garg S, Pilcher CC, Elliott RB, et al. Genetic determination of islet cell autoimmunity in monozygotic twin, dizygotic twin, and non-twin siblings of patients with type 1 diabetes: prospective twin study. BMJ : British Medical Journal. 1999 3;318(7185):698. Available from: /pmc/articles/PMC27778//pmc/articles/PMC27778/?report=abstracthttps://www.ncbi.nlm.nih.gov/pmc/articles/PMC27778/. doi:10.1136/BMJ.318.7185.698.

[22] Hober D, Sauter P. Pathogenesis of type 1 diabetes mellitus: interplay between enterovirus and host. Nature reviews Endocrinology. 2010 5;6(5):279–289. Available from: https://pubmed.ncbi.nlm.nih.gov/20351698/. doi:10.1038/NRENDO.2010.27.

[23] Hober D, Alidjinou EK. Enteroviral pathogenesis of type 1 diabetes: queries and answers. Current opinion in infectious diseases. 2013 6;26(3):263–269. Available from: https://pubmed.ncbi.nlm.nih.gov/23549392/. doi:10.1097/QCO.0B013E3283608300.

[24] Jaïdane H, Sauter P, Sane F, Goffard A, Gharbi J, Hober D. Enteroviruses and type 1 diabetes: towards a better understanding of the relationship. Reviews in medical virology. 2010 9;20(5):265–280. Available from: https://pubmed.ncbi.nlm.nih.gov/20629044/. doi:10.1002/RMV.647.

[25] Schloot NC, Willemen SJM, Duinkerken G, Drijfhout JW, De Vries RRP, Roep BO. Molecular mimicry in type 1 diabetes mellitus revisited: T-cell clones to GAD65 peptides with sequence homology to Coxsackie or proinsulin peptides do not crossreact with homologous counterpart. Human immunology. 2001;62(4):299–309. Available from: https://pubmed.ncbi.nlm.nih.gov/11295462/. doi:10.1016/S0198-8859(01)00223-3.

[26] Dotta F, Censini S, Van Halteren AGS, Marselli L, Masini M, Dionisi S, et al. Coxsackie B4 virus infection of beta cells and natural killer cell insulitis in recent-onset type 1 diabetic patients. Proceedings of the National Academy of Sciences of the United States of America. 2007 3;104(12):5115–5120. Available from: https://pubmed.ncbi.nlm.nih.gov/17360338/. doi:10.1073/PNAS.0700442104.

[27] A H, M S, J W, M M. Childhood vaccination and type 1 diabetes. The New England journal of medicine. 2004 1;350(14):71–72. Available from: https://pubmed.ncbi.nlm.nih.gov/15070789/. doi:10.1056/NEJMOA032665.

[28] Virtanen SM, Rsnen L, kerblom HK, Saukkonen T, Savilahti E, Ylnen K, et al. Diet, cow's milk protein antibodies and the risk of IDDM in Finnish children. Childhood Diabetes in Finland Study Group. Diabetologia. 1994 4;37(4):381–387. Available from: https://pubmed.ncbi.nlm.nih.gov/8063039/. doi:10.1007/S001250050121.

[29] Karlsson MGE, Ludvigsson J. The ABBOS-peptide from bovine serum albumin causes an IFN-gamma and IL-4 mRNA response in lymphocytes from children with recent onset of type 1 diabetes. Diabetes research and clinical practice. 2000;47(3):199–207. Available from: https://pubmed.ncbi.nlm.nih.gov/10741569/. doi:10.1016/S0168-8227(99)00127-8.

[30] Parslow RC, McKinney PA, Law GR, Staines A, Williams R, Bodansky HJ. Incidence of childhood diabetes mellitus in Yorkshire, northern England, is associated with nitrate in drinking water: an ecological analysis. Diabetologia. 1997;40(5):550–556. Available from: https://pubmed.ncbi.nlm.nih.gov/9165223/. doi:10.1007/S001250050714.

[31] Raab J, Giannopoulou EZ, Schneider S, Warncke K, Krasmann M, Winkler C, et al. Prevalence of vitamin D deficiency in pre-type 1 diabetes and its association with disease progression. Diabetologia. 2014;57(5):902–908. Available from: https://pubmed.ncbi.nlm.nih.gov/24531263/. doi:10.1007/S00125-014-3181-4.

[32] Norris JM, Barriga K, Klingensmith G, Hoffman M, Eisenbarth GS, Erlich HA, et al. Timing of initial cereal exposure in infancy and risk of islet autoimmunity. JAMA. 2003 10;290(13):1713–1720. Available from: https://pubmed.ncbi.nlm.nih.gov/14519705/. doi:10.1001/JAMA.290.13.1713.

[33] Norris JM, Yin X, Lamb MM, Barriga K, Seifert J, Hoffman M, et al. Omega-3 polyunsaturated fatty acid intake and islet autoimmunity in children at increased risk for type 1 diabetes. JAMA. 2007 9;298(12):1420–1428. Available from: https://pubmed.ncbi.nlm.nih.gov/17895458/. doi:10.1001/JAMA.298.12.1420.

[34] Li WZ, Stirling K, Yang JJ, Zhang L. Gut microbiota and diabetes: From correlation to causality and mechanism. World Journal of Diabetes. 2020 7;11(7):293. Available from: /pmc/articles/PMC7415231//pmc/articles/PMC7415231/?report=abstracthttps://www.ncbi.nlm.nih.gov/pmc/articles/PMC7415231/. doi:10.4239/WJD.V11.I7.293.

[35] Beyan H, Wen L, Leslie RD. Guts, germs, and meals: the origin of type 1 diabetes. Current diabetes reports. 2012 10;12(5):456–462. Available from: https://pubmed.ncbi.nlm.nih.gov/22753003/. doi:10.1007/S11892-012-0298-Z.

[36] Hu C, Wong FS, Wen L. Type 1 diabetes and gut microbiota: Friend or foe? Pharmacological research. 2015 6;98:9–15. Available from: https://pubmed.ncbi.nlm.nih.gov/25747961/. doi:10.1016/J.PHRS.2015.02.006.

[37] Stene LC, Gale EAM. The prenatal environment and type 1 diabetes. Diabetologia. 2013 9;56(9):1888–1897. Available from: https://pubmed.ncbi.nlm.nih.gov/23657800/. doi:10.1007/S00125-013-2929-6.

[38] Bonifacio E, Warncke K, Winkler C, Wallner M, Ziegler AG. Cesarean section and interferon-induced helicase gene polymorphisms combine to increase childhood type 1 diabetes risk. Diabetes. 2011 12;60(12):3300–3306. Available from: https://pubmed.ncbi.nlm.nih.gov/22110093/. doi:10.2337/DB11-0729.

[39] Lachin JM, Orchard TJ, Nathan DM. Update on cardiovascular outcomes at 30 years of the diabetes control and complications trial/epidemiology of diabetes interventions and complications study. Diabetes care. 2014 1;37(1):39–43. Available from: https://pubmed.ncbi.nlm.nih.gov/24356596/. doi:10.2337/DC13-2116.

[40] Seaquist ER, Anderson J, Childs B, Cryer P, Dagogo-Jack S, Fish L, et al. Hypoglycemia and diabetes: a report of a workgroup of the American Diabetes Association and the Endocrine Society. Diabetes care. 2013 5;36(5):1384–1395. Available from: https://pubmed.ncbi.nlm.nih.gov/23589542/. doi:10.2337/DC12-2480.

[41] AM J, G M, CM R, N S, P C, B W, et al. Long-term effect of diabetes and its treatment on cognitive function. The New England journal of medicine. 2007 5;356(18):1842–1852. Available from: https://pubmed.ncbi.nlm.nih.gov/17476010/. doi:10.1056/NEJMOA066397.

[42] Patterson CC, Dahlquist G, Harjutsalo V, Joner G, Feltbower RG, Svensson J, et al. Early mortality in EURODIAB population-based cohorts of type 1 diabetes diagnosed in childhood since 1989. Diabetologia. 2007;50(12):2439–2442. Available from: https://pubmed.ncbi.nlm.nih.gov/17901942/. doi:10.1007/S00125-007-0824-8.

[43] Huo L, Shaw JE, Wong E, Harding JL, Peeters A, Magliano DJ. Burden of diabetes in Australia: life expectancy and disability-free life expectancy in adults with diabetes. Diabetologia. 2016 7;59(7):1437–1445. Available from: https://pubmed.ncbi.nlm.nih.gov/27075450/. doi:10.1007/S00125-016-3948-X.

[44] Whittemore R, Jaser S, Chao A, Jang M, Grey M. Psychological experience of parents of children with type 1 diabetes: a systematic mixed-studies review. The Diabetes educator. 2012;38(4):562–579. Available from: https://pubmed.ncbi.nlm.nih.gov/22581804/. doi:10.1177/0145721712445216.

[45] Van Name MA, Hilliard ME, Boyle CT, Miller KM, DeSalvo DJ, Anderson BJ, et al. Nighttime is the worst time: Parental fear of hypoglycemia in young children with type 1 diabetes. Pediatric diabetes. 2018 2;19(1):114–120. Available from: https://pubmed.ncbi.nlm.nih.gov/28429581/. doi:10.1111/PEDI.12525.

[46] Mobasseri M, Shirmohammadi M, Amiri T, Vahed N, Fard HH, Ghojazadeh M. Prevalence and incidence of type 1 diabetes in the world: a systematic review and meta-analysis. Health Promotion Perspectives. 2020;10(2):98. Available from: /pmc/articles/PMC7146037//pmc/articles/PMC7146037/?report=abstracthttps://www.ncbi.nlm.nih.gov/pmc/articles/PMC7146037/. doi:10.34172/HPP.2020.18.

[47] Stoffers DA. The development of beta-cell mass: recent progress and potential role of GLP-1. Hormone and metabolic research = Hormon- und Stoffwechselforschung = Hormones et metabolisme. 2004 11;36(11-12):811–821. Available from: https://pubmed.ncbi.nlm.nih.gov/15655713/. doi:10.1055/S-2004-826168.

[48] Lawrence JM, Divers J, Isom S, Saydah S, Imperatore G, Pihoker C, et al. Trends in Prevalence of Type 1 and Type 2 Diabetes in Children and Adolescents in the US, 2001-2017. JAMA. 2021 8;326(8):717–727. Available from: https://jamanetwork.com/journals/jama/fullarticle/2783420. doi:10.1001/JAMA.2021.11165.

[49] Gestational diabetes - NHS;. Available from: https://www.nhs.uk/conditions/gestational-diabetes/.

[50] Diabetes - NHS;. Available from: https://www.nhs.uk/conditions/diabetes/.

[51] Frederick G. Banting Nobel Lecture; 1925.

[52] Evans M, Schumm-Draeger PM, Vora J, King AB. A review of modern insulin analogue pharmacokinetic and pharmacodynamic profiles in type 2 diabetes: improvements and limitations. Diabetes, obesity & metabolism. 2011;13(8):677–684. Available from: https://pubmed.ncbi.nlm.nih.gov/21410860/. doi:10.1111/J.1463-1326.2011.01395.X.

[53] Rios Y, García-Rodríguez J, Sanchez E, Alanis A, Ruiz-Velázquez E, Pardo A. Comparative effectiveness and safety of methods of insulin delivery and glucose monitoring for diabetes mellitus: a systematic review and meta-analysis. Annals of internal medicine. 2012;157(5):390–400. Available from: https://pubmed.ncbi.nlm.nih.gov/22777524/. doi:10.7326/0003-4819-157-5-201209040-00508.

[54] Pathak V, Pathak NM, O'Neill CL, Guduric-Fuchs J, Medina RJ. Therapies for Type 1 Diabetes: Current Scenario and Future Perspectives. Clinical Medicine Insights Endocrinology and Diabetes. 2019 5;12. Available from: /pmc/articles/PMC6501476//pmc/articles/PMC6501476/?report=abstracthttps://www.ncbi.nlm.nih.gov/pmc/articles/PMC6501476/. doi:10.1177/1179551419844521.

[55] Abramson A, Caffarel-Salvador E, Khang M, Dellal D, Silverstein D, Gao Y, et al. An ingestible self-orienting system for oral delivery of macromolecules. Science (New York, NY). 2019 2;363(6427):611–615. Available from: https://pubmed.ncbi.nlm.nih.gov/30733413/. doi:10.1126/SCIENCE.AAU2277.

[56] Piłaciński S, Zozulińska-Ziółkiewicz DA. Influence of lifestyle on the course of type 1 diabetes mellitus. Archives of Medical Science : AMS. 2014 2;10(1):124. Available from: /pmc/articles/PMC3953982//pmc/articles/PMC3953982/?report=abstracthttps://www.ncbi.nlm.nih.gov/pmc/articles/PMC3953982/. doi:10.5114/AOMS.2014.40739.

[57] How long is the wait for a pancreas? - Organ transplantation - NHS Blood and Transplant;. Available from: https://www.nhsbt.nhs.uk/organ-transplantation/pancreas/receiving-a-pancreas/how-long-is-the-wait-for-a-pancreas/.

[58] Gheith O, Farouk N, Nampoory N, Halim MA, Al-Otaibi T. Diabetic kidney disease: world wide difference of prevalence and risk factors. Journal of Nephropharmacology. 2016;5(1):49. Available from: /pmc/articles/PMC5297507//pmc/articles/PMC5297507/?report=abstracthttps://www.ncbi.nlm.nih.gov/pmc/articles/PMC5297507/.

[59] Bellin MD, Dunn TB. Transplant strategies for type 1 diabetes: whole pancreas, islet and porcine beta cell therapies. Diabetologia. 2020 10;63(10):2049–2056. Available from: https://pubmed.ncbi.nlm.nih.gov/32894315/. doi:10.1007/S00125-020-05184-7.

[60] Ricordi C, Lacy PE, Finke EH, Olack BJ, Scharp DW. Automated method for isolation of human pancreatic islets. Diabetes. 1988;37(4):413–420. Available from: https://pubmed.ncbi.nlm.nih.gov/3288530/. doi:10.2337/DIAB.37.4.413.

[61] Shapiro AMJ, Lakey JRT, Ryan EA, Korbutt GS, Toth E, Warnock GL, et al. Islet transplantation in seven patients with type 1 diabetes mellitus using a glucocorticoid-free immunosuppressive regimen. The New England journal of medicine. 2000 7;343(4):230–238. Available from: https://pubmed.ncbi.nlm.nih.gov/10911004/. doi:10.1056/NEJM200007273430401.

[62] Bottino R, Knoll MF, Knoll CA, Bertera S, Trucco MM. The Future of Islet Transplantation Is Now. Frontiers in medicine. 2018;5(JUL). Available from: https://pubmed.ncbi.nlm.nih.gov/30057900/. doi:10.3389/FMED.2018.00202.

[63] Shapiro AMJ, Pokrywczynska M, Ricordi C. Clinical pancreatic islet transplantation. Nature reviews Endocrinology. 2017 5;13(5):268–277. Available from: https://pubmed.ncbi.nlm.nih.gov/27834384/. doi:10.1038/NRENDO.2016.178.

[64] Vantyghem MC, de Koning EJP, Pattou F, Rickels MR. Advances in β-cell replacement therapy for the treatment of type 1 diabetes. Lancet (London, England). 2019 10;394(10205):1274–1285. Available from: https://pubmed.ncbi.nlm.nih.gov/31533905/. doi:10.1016/S0140-6736(19)31334-0.

[65] Korsgren O. Islet Encapsulation: Physiological Possibilities and Limitations. Diabetes. 2017 7;66(7):1748–1754. Available from: https://pubmed.ncbi.nlm.nih.gov/28637827/. doi:10.2337/DB17-0065.

[66] Desai TA, Tang Q. Islet encapsulation therapy - racing towards the finish line? Nature reviews Endocrinology. 2018 11;14(11):630–632. Available from: https://pubmed.ncbi.nlm.nih.gov/30275463/. doi:10.1038/S41574-018-0100-7.

[67] Liu W, Wang Y, Wang J, Lanier OL, Wechsler ME, Peppas NA, et al. Macroencapsulation Devices for Cell Therapy. Engineering. 2022 6;13:53–70. doi:10.1016/J.ENG.2021.10.021.

[68] Espona-Noguera A, Ciriza J, Cañibano-Hernández A, Orive G, Hernández RM, Del Burgo LS, et al. Review of Advanced Hydrogel-Based Cell Encapsulation Systems for Insulin Delivery in Type 1 Diabetes Mellitus. Pharmaceutics. 2019 11;11(11). Available from: https://pubmed.ncbi.nlm.nih.gov/31726670/. doi:10.3390/PHARMACEUTICS11110597.

[69] Ernst AU, Bowers DT, Wang LH, Shariati K, Plesser MD, Brown NK, et al. Nanotechnology in cell replacement therapies for type 1 diabetes. Advanced Drug Delivery Reviews. 2019 1;139:116–138. doi:10.1016/J.ADDR.2019.01.013.

[70] Bowers DT, Song W, Wang LH, Ma M. Engineering the vasculature for islet transplantation. Acta Biomaterialia. 2019 9;95:131–151. doi:10.1016/J.ACTBIO.2019.05.051.

[71] Zhi ZL, Khan F, Pickup JC. Multilayer nanoencapsulation: a nanomedicine technology for diabetes research and management. Diabetes research and clinical practice. 2013 5;100(2):162–169. Available from: https://pubmed.ncbi.nlm.nih.gov/23273839/. doi:10.1016/J.DIABRES.2012.11.027.

[72] Kizilel S, Scavone A, Liu X, Nothias JM, Ostrega D, Witkowski P, et al. Encapsulation of pancreatic islets within nano-thin functional polyethylene glycol coatings for enhanced insulin secretion. Tissue engineering Part A. 2010 7;16(7):2217–2228. Available from: https://pubmed.ncbi.nlm.nih.gov/20163204/. doi:10.1089/TEN.TEA.2009.0640.

[73] Wilson JT, Cui W, Chaikof EL. Layer-by-layer assembly of a conformal nanothin PEG coating for intraportal islet transplantation. Nano letters. 2008 7;8(7):1940–1948. Available from: https://pubmed.ncbi.nlm.nih.gov/18547122/. doi:10.1021/NL080694Q.

[74] Dimitrioglou N, Kanelli M, Papageorgiou E, Karatzas T, Hatziavramidis D. Paving the way for successful islet encapsulation. Drug discovery today. 2019 3;24(3):737–748. Available from: https://pubmed.ncbi.nlm.nih.gov/30738185/. doi:10.1016/J.DRUDIS.2019.01.020.

[75] Pérez-Luna VH, González-Reynoso O. Encapsulation of Biological Agents in Hydrogels for Therapeutic Applications. Gels (Basel, Switzerland). 2018 9;4(3). Available from: https://pubmed.ncbi.nlm.nih.gov/30674837/. doi:10.3390/GELS4030061.

[76] White AM, Shamul JG, Xu J, Stewart S, Bromberg JS, He X. Engineering Strategies to Improve Islet Transplantation for Type 1 Diabetes Therapy. ACS biomaterials science & engineering. 2020 5;6(5):2543–2562. Available from: https://pubmed.ncbi.nlm.nih.gov/33299929/. doi:10.1021/ACSBIOMATERIALS.9B01406.

[77] Omami M, McGarrigle JJ, Reedy M, Isa D, Ghani S, Marchese E, et al. Islet Microencapsulation: Strategies and Clinical Status in Diabetes. Current diabetes reports. 2017 7;17(7). Available from: https://pubmed.ncbi.nlm.nih.gov/28523592/. doi:10.1007/S11892-017-0877-0.

[78] Lim F, Sun AM. Microencapsulated islets as bioartificial endocrine pancreas. Science (New York, NY). 1980;210(4472):908–910. Available from: https://pubmed.ncbi.nlm.nih.gov/6776628/. doi:10.1126/SCIENCE.6776628.

[79] Moreira A, Carneiro J, Campos JBLM, Miranda JM. Production of hydrogel microparticles in microfluidic devices: a review. Microfluidics and Nanofluidics. 2021 2;25(2). doi:10.1007/S10404-020-02413-8.

[80] Fitzgerald KA, Malhotra M, Curtin CM, O'Brien FJ, O'Driscoll CM. Life in 3D is never flat: 3D models to optimise drug delivery. Journal of controlled release : official journal of the Controlled Release Society. 2015 10;215:39–54. Available from: https://pubmed.ncbi.nlm.nih.gov/26220617/. doi:10.1016/J.JCONREL.2015.07.020.

[81] Shamir ER, Ewald AJ. Three-dimensional organotypic culture: experimental models of mammalian biology and disease. Nature reviews Molecular cell biology. 2014 1;15(10):647. Available from: /pmc/articles/PMC4352326//pmc/articles/PMC4352326/?report=abstracthttps://www.ncbi.nlm.nih.gov/pmc/articles/PMC4352326/. doi:10.1038/NRM3873.

[82] Correia CR, Bjørge IM, Zeng J, Matsusaki M, Mano JF. Liquefied Microcapsules as Dual-Microcarriers for 3D+3D Bottom-Up Tissue Engineering. Advanced healthcare materials. 2019 11;8(22). Available from: https://pubmed.ncbi.nlm.nih.gov/31603632/. doi:10.1002/ADHM.201901221.

[83] Yu L, Ni C, Grist SM, Bayly C, Cheung KC. Alginate core-shell beads for simplified three-dimensional tumor spheroid culture and drug screening. Biomedical microdevices. 2015 4;17(2). Available from: https://pubmed.ncbi.nlm.nih.gov/25681969/. doi:10.1007/S10544-014-9918-5.

[84] van Loo B, Salehi SS, Henke S, Shamloo A, Kamperman T, Karperien M, et al. Enzymatic outside-in cross-linking enables single-step microcapsule production for high-throughput three-dimensional cell microaggregate formation. Materials Today Bio. 2020 3;6. doi:10.1016/J.MTBIO.2020.100047.

[85] Selimović Oh J, Bae H, Dokmeci M, Khademhosseini A. Microscale Strategies for Generating Cell-Encapsulating Hydrogels. Polymers. 2012;4(3):1554–1579. Available from: https://pubmed.ncbi.nlm.nih.gov/23626908/. doi:10.3390/POLYM4031554.

[86] Lopez-Mendez TB, Santos-Vizcaino E, Pedraz JL, Hernandez RM, Orive G. Cell microencapsulation technologies for sustained drug delivery: Clinical trials and companies. Drug discovery today. 2021 3;26(3):852–861. Available from: https://pubmed.ncbi.nlm.nih.gov/33242694/. doi:10.1016/J.DRUDIS.2020.11.019.

[87] Reis RL. Encyclopedia of tissue engineering and regenerative medicine.

[88] Knobeloch T, Abadi SEM, Bruns J, Zustiak SP, Kwon G. Injectable Polyethylene Glycol Hydrogel for Islet Encapsulation: an in vitro and in vivo Characterization. Biomedical physics & engineering express. 2017 6;3(3):035022. Available from: /pmc/articles/PMC5842952//pmc/articles/PMC5842952/?report=abstracthttps://www.ncbi.nlm.nih.gov/pmc/articles/PMC5842952/. doi:10.1088/2057-1976/AA742B.

[89] Weaver JD, Headen DM, Coronel MM, Hunckler MD, Shirwan H, García AJ. Synthetic poly(ethylene glycol)-based microfluidic islet encapsulation reduces graft volume for delivery to highly vascularized and retrievable transplant site. American Journal of Transplantation. 2019 5;19(5):1315–1327. Available from: https://onlinelibrary.wiley.com/doi/full/10.1111/ajt.15168https://onlinelibrary.wiley.com/doi/abs/10.1111/ajt.15168https://onlinelibrary.wiley.com/doi/10.1111/ajt.15168. doi:10.1111/AJT.15168.

[90] De Vos P, Lazarjani HA, Poncelet D, Faas MM. Polymers in cell encapsulation from an enveloped cell perspective. Advanced drug delivery reviews. 2014 4;67-68:15–34. Available from: https://pubmed.ncbi.nlm.nih.gov/24270009/. doi:10.1016/J.ADDR.2013.11.005.

[91] Truong NF, Kurt E, Tahmizyan N, Lesher-Pérez SC, Chen M, Darling NJ, et al. Microporous annealed particle hydrogel stiffness, void space size, and adhesion properties impact cell proliferation, cell spreading, and gene transfer. Acta Biomaterialia. 2019 8;94:160–172. doi:10.1016/J.ACTBIO.2019.02.054.

[92] Pruett L, Koehn H, Martz T, Churnin I, Ferrante S, Salopek L, et al. Development of a microporous annealed particle hydrogel for long-term vocal fold augmentation. The Laryngoscope. 2020 10;130(10):2432–2441. Available from: https://pubmed.ncbi.nlm.nih.gov/31821567/. doi:10.1002/LARY.28442.

[93] Paggi CA, Venzac B, Karperien M, Leijten JCH, Le Gac S. Monolithic microfluidic platform for exerting gradients of compression on cell-laden hydrogels, and application to a model of the articular cartilage. Sensors and Actuators B: Chemical. 2020 7;315:127917. doi:10.1016/J.SNB.2020.127917.

[94] Rommel D, Mork M, Vedaraman S, Bastard C, Guerzoni LPB, Kittel Y, et al. Functionalized Microgel Rods Interlinked into Soft Macroporous Structures for 3D Cell Culture. Advanced Science. 2022 4;9(10). Available from: /pmc/articles/PMC8981485//pmc/articles/PMC8981485/?report=abstracthttps://www.ncbi.nlm.nih.gov/pmc/articles/PMC8981485/. doi:10.1002/ADVS.202103554.

[95] Liu L, Yuan Y, Deng W, Li S. Determining random packing density and equivalent packing size of superballs via binary mixtures with spheres. Available from: https://doi.org/10.1016/j.ces.2019.03.041. doi:10.1016/j.ces.2019.03.041.

[96] Suszynski TM, Wilhelm JJ, Radosevich DM, Balamurugan AN, Sutherland DER, Beilman GJ, et al. Islet Size Index as a Predictor of Outcomes in Clinical Islet Autotransplantation. Transplantation. 2014 6;97(12):1286. Available from: /pmc/articles/PMC4682552//pmc/articles/PMC4682552/?report=abstracthttps://www.ncbi.nlm.nih.gov/pmc/articles/PMC4682552/. doi:10.1097/01.TP.0000441873.35383.1E.

[97] Huang HH, Harrington S, Stehno-Bittel L. The Flaws and Future of Islet Volume Measurements. Cell Transplantation. 2018 7;27(7):1017. Available from: /pmc/articles/PMC6158542//pmc/articles/PMC6158542/?report=abstracthttps://www.ncbi.nlm.nih.gov/pmc/articles/PMC6158542/. doi:10.1177/0963689718779898.

[98] Huang E, Peng N, Xiao F, Hu D, Wang X, Lu L. The Roles of Immune Cells in the Pathogenesis of Fibrosis. International Journal of Molecular Sciences. 2020 8;21(15):1–27. Available from: /pmc/articles/PMC7432671//pmc/articles/PMC7432671/?report=abstracthttps://www.ncbi.nlm.nih.gov/pmc/articles/PMC7432671/. doi:10.3390/IJMS21155203.

[99] Cheng K, de lghingaro Augusto V, Nolan CJ, Turner N, Hallahan N, Andrikopoulos S, et al. High Passage MIN6 Cells Have Impaired Insulin Secretion with Impaired Glucose and Lipid Oxidation. PLOS ONE. 2012 7;7(7):e40868. Available from: https://journals.plos.org/plosone/article?id=10.1371/journal.pone.0040868. doi:10.1371/JOURNAL.PONE.0040868.